STABILIZATION OF PARALLELED STATIC- AND AMPLIDYNE-EXCITED SYNCHRONOUS MACHINES

A Thesis

Presented to

the Faculty of Graduate Studies and Research

University of Manitoba

In Partial Fulfillment

of the Requirements for the Degree

Master of Science in Electrical Engineering

---

by

Satish Sud

May 1969

ABSTRACT

In this thesis it is attempted to compare the effect of various kinds of stabilizer signals on the dynamic and the transient stabilities of two paralleled static and amplidyne excited synchronous machines. A simplified linear model of the system is analysed and then a more complicated model of the system is simulated. The IBM-360/65 Digital Computer was used to simulate the model of the system and it is shown that the speed error, the derivative of the terminal voltage, and the accelerating power signals are the most suitable for effecting a stabilization.

ACKNOWLEDGEMENT

The author wishes to acknowledge his indebtedness to Professor G. W. Swift for his never failing guidance and assistance and to Professor M. Z. Tarnawecky for his interest and encouragement. The author also wishes to thank Manitoba Hydro for having provided the necessary information. Thanks are due to Miss L. Milkowski for the expertly typed manuscript.

The financial assistance from N.R.C. under grant number A2780, is also acknowledged.

TO MY PARENTS

WITH DEEP GRATITUDE AND AFFECTION

TABLE OF CONTENTS

LIST OF TABLES

PAGE

LIST OF ILLUSTRATIONS

I. INTRODUCTION

Stability problems should not force operators to run a station at less than its rated capacity. To achieve this one must ensure dynamic and transient stabilities when working at high loads. Optimization of the excitation system was recommended as a means to achieving an improvement in the performance of transmission systems [18,19].* High speed excitation systems were introduced and found to be successful [10,12]. It was also found that dynamic and transient stabilities could be improved by using stabilizer signals [1-4,6,10-13,17]. The various authors recommend different kinds of stabilizer signals such as:

(a) Speed error signal ($\Delta\omega_2$),

(b) Rate of change of Field Current signal (sI_f),

(c) Rate of change of Terminal Voltage signal (sV_{t2}),

(d) Rate of change of Field Voltage signal (sV_f),

(e) Rate of change of Reactive Power signal (sQ_u),

(f) Rate of change of Active Power signal (sP_u),

(g) Rate of change of Active and Reactive Power signal (sK_pPu+sK_qQu),

and a variety of other feedback signals. Symbols are listed in Appendix D.

This thesis describes the research undertaken to establish which feedback signal is most suitable, if indeed there is one.

To keep the problem as practical as possible, it was decided to model the Grand Rapids Power Generating Station of Manitoba Hydro along with the transmission system to Ashern. At Grand Rapids there are four generators, two of which have static excitation; the other two have conventional amplidyne excitation. The generator, system, and automatic

---

*Bracketted [] numbers refer to Bibliography.

voltage regulator parameters used were those provided by Manitoba Hydro. Two of the generators - one with static excitation and the other with conventional amplidyne excitation - were actually represented in the system model. A single line representation of the system is shown in Figure 1.

The criteria chosen for determining the stability were the same as those used by Manitoba Hydro for their Grand Rapids Station. For dynamic stability the system is to remain stable for a 3.5% change in the reference voltage, and for transient stability the system must remain stable when one of the two transmission lines between Grand Rapids and Ashern is switched out. Two other transmission lines also exist [19].

Mode of Operation of the Stabilizer Signal

A disturbance in a power system causes an oscillation in the electrical angles of the machines connected to the system. The peak of the power angle curve may be reduced due to the disturbance which may also cause the terminal voltage to drop and hence affect the power transmitted.

The terminal voltage should be increased in magnitude during the time that the angle between the terminal voltage and the receiving end voltage is increasing and conversely decreased while the angle is decreasing. This will tend to cause more power to be transferred when the voltage is increased and less power to be transferred when the voltage is decreased. The net effect is intended to damp the oscillations of the electrical angles of the machines.

The increase and decrease in the terminal voltage is effected by means of a stabilizer signal which helps balance the accelerating power of the rotor. The signal must be such that it acts on the excitation

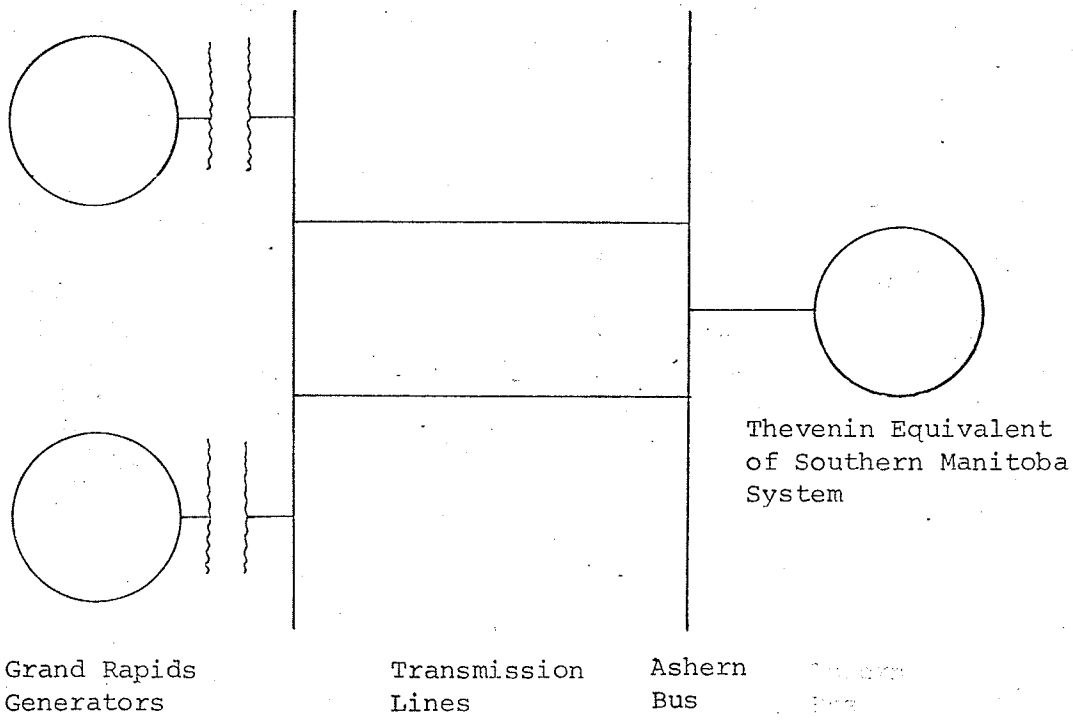

Figure 1. Single Line Diagram of the System

system at the right time and in the right direction i.e. its polarity must be such as to increase the excitation when power transfer is decreasing and to decrease the excitation when the power transfer is increasing.

During a disturbance the synchronizing torque generated in a machine is approximately inversely proportional to the transient reactance. Consequently the stability is improved as the transient reactance is reduced. By a subsidiary feedback, called the stabilizer signal, the reactance is in effect reduced during the transient and so there is a contribution to the system damping.

II. A LINEAR MODEL

The Heffron and Phillips Model

An analysis of dynamic stability is attempted assuming operation in the linear region, and using the Heffron and Phillips approximate model [9,14]. To avoid a very complicated analysis, a simplified system is considered in which there is one machine with static excitation feeding power to an infinite bus. A block diagram of the model is shown in Figure 2, and a phasor diagram is shown in Figure 3.

The constants $K_1 - K_6$ are the Heffron and Phillips constants which may be calculated as follows:

$$K_1 = (V_{go}V_b\cos\delta_o)/(x_q + x_t) + (V_{dmo}V_b\sin\delta_o)(1 - x_d''/x_q)/(x_d' + x_t) \tag{2.1}$$

$$K_2 = (V_b\sin\delta_o)/(x_d' + x_t) \tag{2.2}$$

$$K_3 = (x_d' + x_t)/(x_d + x_t) \tag{2.3}$$

$$K_4 = (x_d - x_d')(V_b\sin\delta_o)/(x_d + x_t) \tag{2.4}$$

$$K_5 = (V_{dmo}/V_{to})(x_qV_b\cos\delta_o)/(x_q + x_t) - (V_{qmo}/V_{to})(x_d'V_b\sin\delta_o)/(x_d' + x_t) \tag{2.5}$$

$$K_6 = (V_{qmo}/V_{to})x_t/(x_d' + x_t) \tag{2.6}$$

The zero subscripts indicate an operating point and the Heffron and Phillips constants are for small deviations from that operating point.

A machine with static excitation having a high gain in the feedback loop is considered so the value of the excitation system time constant can be assumed to be negligibly small. A few of the signals which proved to be satisfactory in the more complicated model are discussed. The stabilizer signals are added to the linear model as shown

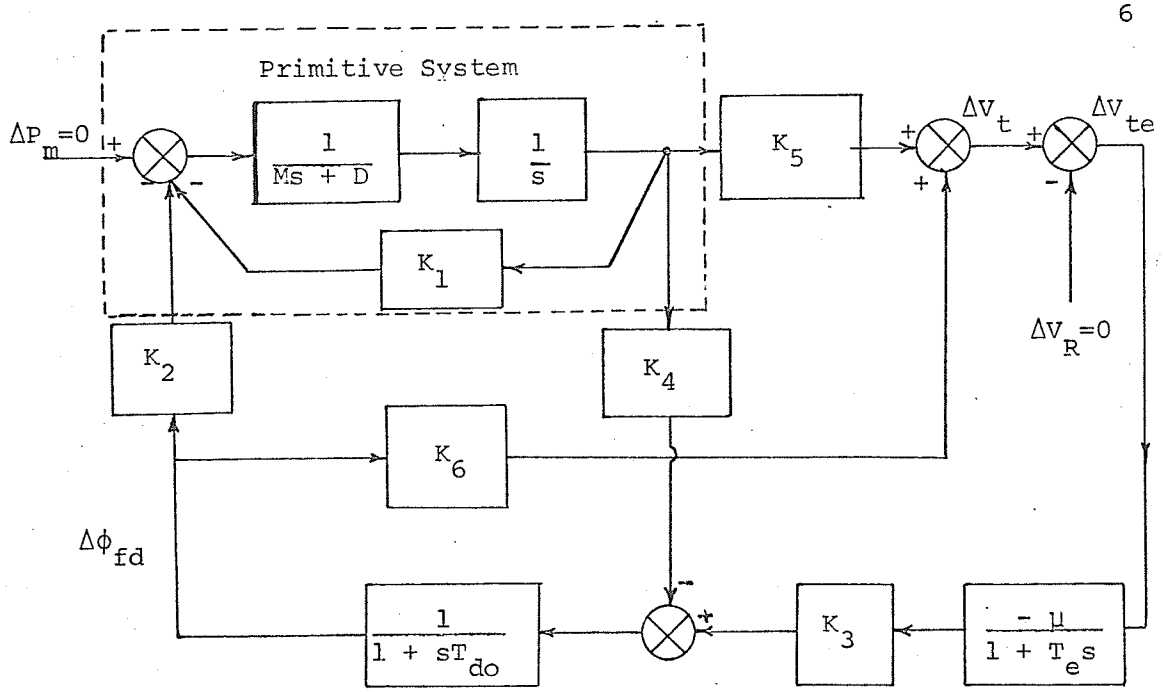

Figure 2. The Heffron and Phillips Model

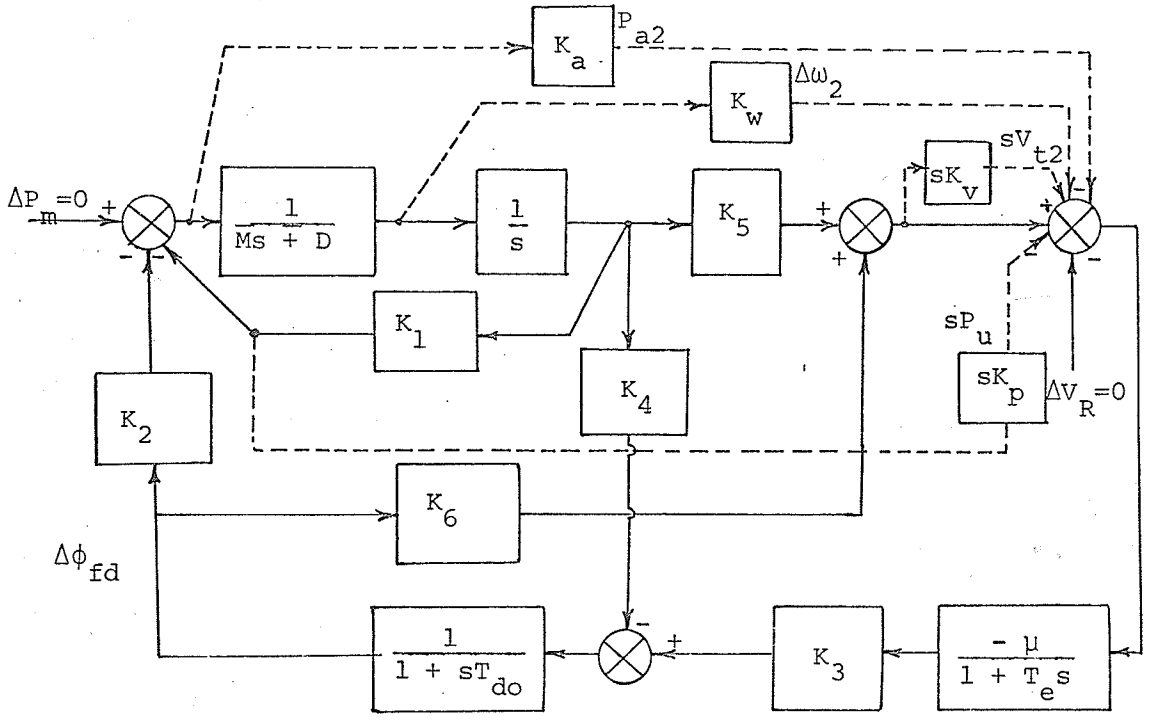

Figure 2a. Model Showing Stabilizer Signals

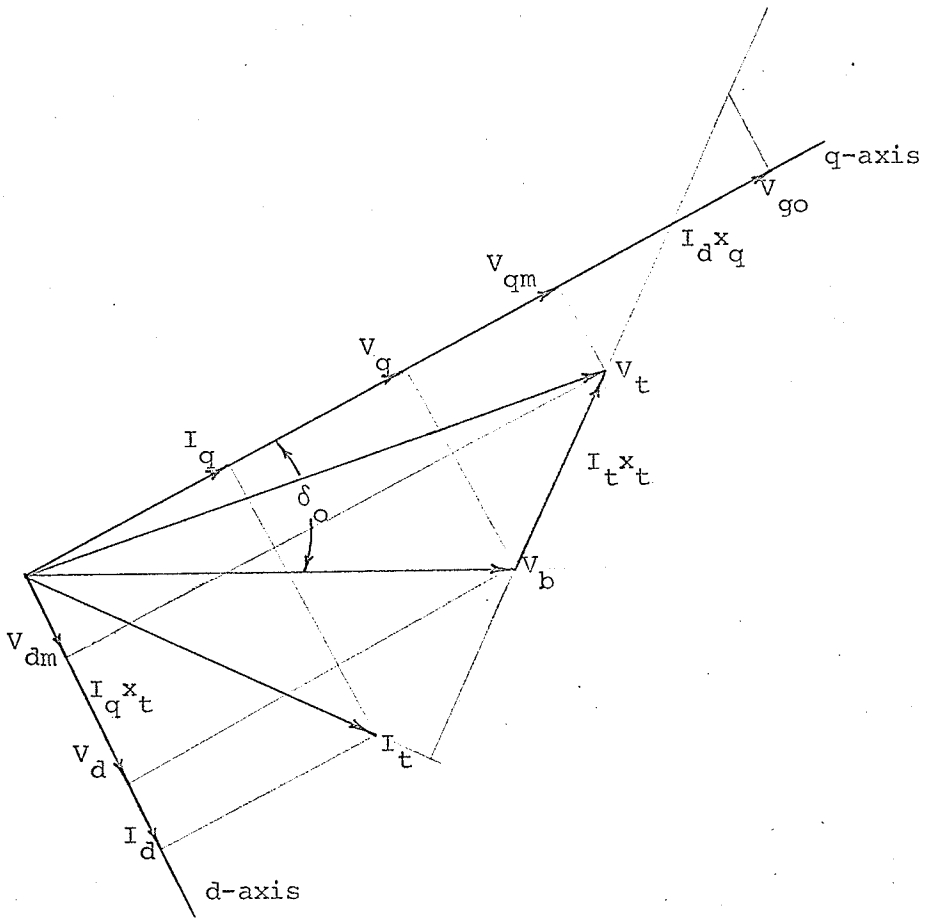

Figure 3. Phasor Diagram for the Generator

in Figure 2a.

Analysis of the Parametric Root Locus

The characteristic equation of the autonomous system with no stabilizer is first derived. Rearrangement of equations

$$(Ms^2 + Ds)\Delta\delta = - K_1\Delta\delta - K_2\Delta\phi_{fd} \tag{2.7}$$

$$\Delta\phi_{fd} = (-\mu K_3\Delta V_{te} - K_4\Delta\delta)/(1 + sT_{do}) \tag{2.8}$$

$$\Delta V_{te} = K_6\Delta\phi_{fd} + K_5\Delta\delta \tag{2.9}$$

produces

$$(Ms^2 + Ds + K_1)\Delta\delta + K_2\Delta\phi_{fd} + 0.\Delta V_{te} = 0 \tag{2.10}$$

$$K_4\Delta\delta + (1 + sT_{do})\Delta\phi_{fd} + K_3\Delta V_{te} = 0 \tag{2.11}$$

$$- K_5\Delta\delta - K_6\Delta\phi_{fd} + \Delta V_{te} = 0 \tag{2.12}$$

or in the matrix form

$$\begin{bmatrix} Ms^2 + Ds + K_1 & K_2 & 0 \\ K_4 & 1 + sT_{do} & \mu K_3 \\ - K_5 & - K_6 & 1 \end{bmatrix} \begin{bmatrix} \Delta\delta \\ \Delta\phi_{fd} \\ \Delta V_{te} \end{bmatrix} = 0 \tag{2.13}$$

and the determinant of the coefficient matrix is

$$\begin{aligned} & s^3MT_{do} + s^2\{DT_{do} + M(1 + \mu K_3K_6)\} \\ & + s\{K_1T_{do} + D(1 + \mu K_3K_6)\} \\ & + \{K_1(1 + \mu K_3K_6) - K_2(K_4 + \mu K_3K_5)\} \end{aligned} \tag{2.14}$$

The characteristic equation of the system with the $\Delta\omega_2$ stabilizer is determined from equations (2.7), (2.8), and

$$\Delta V_{te} = K_6\Delta\phi_{fd} + K_5\Delta\delta - sK_w\Delta\delta \tag{2.15}$$

in the place of (2.9).

In the matrix form these become

$$\begin{bmatrix} Ms^2 + Ds + K_1 & 0 \\ K_4 & 1 + sT_{do} \quad \mu K_3 \\ sK_w - K_5 & -K_6 \quad 1 \end{bmatrix} \begin{bmatrix} \Delta\delta \\ \Delta\phi_{fd} \\ \Delta V_{te} \end{bmatrix} = 0 \tag{2.16}$$

the characteristic equation of which is

$$\begin{aligned} & s^3 MT_{do} + s^2\{DT_{do} + M(1 + \mu K_3 K_6)\} \\ & + s\{K_1 T_{do} + D(1 + \mu K_3 K_6) + \mu K_2 K_3 K_w\} \\ & + \{K_1(1 + \mu K_3 K_6) - K_2(K_4 + \mu K_3 K_5)\} = 0 \end{aligned} \tag{2.17}$$

It is quite apparent from the simplified model that the speed error signal, $\Delta\omega_2$, is identical to the signal obtained from the derivative of the active power if

$$K_w = K_1 K_p \tag{2.18}$$

Thus with this substitution the characteristic equation using the sP_u signal in place of the $\Delta\omega_2$ signal becomes

$$\begin{aligned} & s^3 MT_{do} + s^2\{DT_{do} + M(1 + \mu K_3 K_6)\} \\ & + s\{K_1 T_{do} + D(1 + \mu K_3 K_6) + \mu K_1 K_2 K_3 K_p\} \\ & + \{K_1(1 + \mu K_3 K_6) - K_2(K_4 + \mu K_3 K_5)\} = 0 \end{aligned} \tag{2.19}$$

The parametric root locus for variable K_p or K_w with either the $\Delta\omega_2$ or the sP_u stabilizer respectively is shown in Figure 4 for typical values of the constants, with the regulator gain large. From this it can be seen that by using the appropriate value of the gain K_p or K_w an increased damping can be obtained thereby improving the stability. The parametric root locus of the two systems being identical it appears that what could be accomplished with one should be accomplishable with the other. This was, however, not borne out by simulations on the more

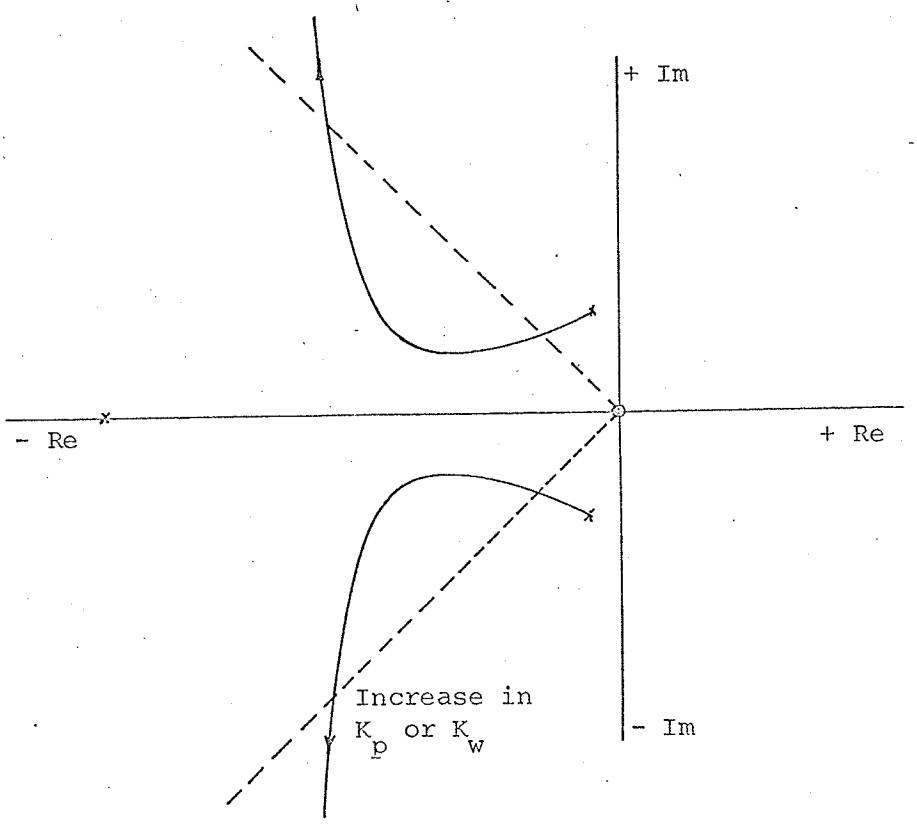

Figure 4. Parametric Root Locus with the sP_u or the $\Delta\omega_2$ Stabilizer Signal

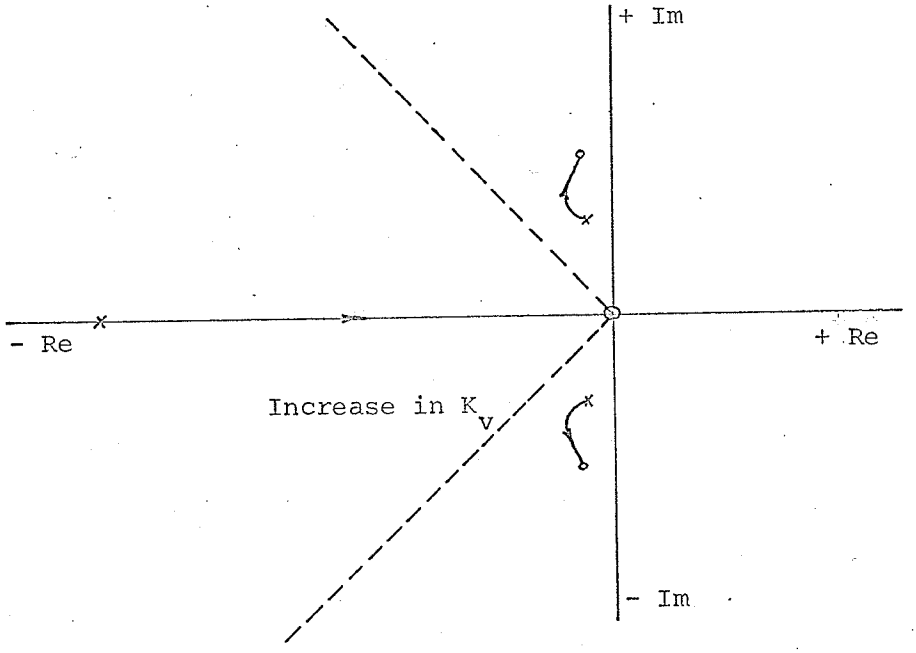

Figure 5. Parametric Root Locus with the sV_{t2} Stabilizer Signal

complicated model.

The characteristic equation for the system with sV_{t2} stabilizer is determined by using equation (2.7), (2.8), and

$$\Delta V_{te} = (K_6\Delta\phi_{fd} + K_5\Delta\delta)(1 + sK_v) \tag{2.20}$$

These in the matrix form become

$$\begin{bmatrix} Ms^2 + Ds + K_1 & K_2 & 0 \\ K_1 & (1 + sT_{do}) & \mu K_3 \\ -K_5(1 + sK_v) & -K_6(1 + sK_v) & 1 \end{bmatrix} \begin{bmatrix} \Delta\delta \\ \Delta\phi_{fd} \\ \Delta V_{te} \end{bmatrix} = 0 \tag{2.21}$$

which has the characteristic equation

$$\begin{aligned} &s^3(MT_{do} + \mu MK_3K_6K_v) + s^2\{DT_{do} + M(1 + \mu K_3K_6) + \mu DK_3K_6K_v\} \\ &+ s^1\{K_1T_{do} + D(1 + \mu K_3K_6) + \mu K_3K_v(K_1K_6 - K_2K_5)\} \\ &+ \{K_1(1 + \mu K_3K_6) - K_2(K_4 + \mu K_3K_5)\} = 0 \end{aligned} \tag{2.22}$$

The sV_{t2} signal changes the characteristic equation significantly. By observing the parametric root locus with such an sV_{t2} stabilizer it is seen that in effect the signal introduces a pair of zeros which are the solutions of the equation

$$s(MK_6s^2 + DK_6s + K_1K_6 - K_2K_5) = 0 \tag{2.23}$$

so that the zeros introduced are the solutions of the quadratic equation

$$s^2 + (D/M)s + (K_1/M - K_2K_5/MK_6) = 0 \tag{2.24}$$

having an undamped natural frequency

$$w_n = \sqrt{K_1/M - K_2K_5/MK_6} \tag{2.25}$$

It is interesting to note that this natural frequency is only slightly different from that of the "primitive system" (See Figure 2)

$$s^2 + (D/M)s + (K_1/M) = 0 \tag{2.26}$$

which has the natural frequency

$$w_n = \sqrt{K_1/M} \tag{2.27}$$

From the parametric root locus shown in Figure 5 it is not at all apparent how the sV_{t2} signal introduces damping so as to improve dynamic stability. However, in the sV_{t2} signal a component similar to the $\Delta\omega_2$ signal is recognizable. The $\Delta\omega_2$ signal is fed back directly to the voltage regulator, so that the signal fed back is $-K_w\Delta\dot{\delta}$. In the case of the sV_{t2} signal, the signal fed back is $K_v\{K_5 - K_4K_6/(1 + sT_{do})\}\Delta\dot{\delta}$. Now K_5 is negative for high loads and is of such magnitude that it dominates the term $\{K_4K_6/(1 + sT_{do})\}$ for the low frequency variations that take place in the system, so that effectively we are feeding back $K_5K_v\Delta\dot{\delta}$. Thus the sV_{t2} signal has the same polarity and form as that of the $\Delta\omega_2$ signal. Although the above is not a rigorous justification for the action of the sV_{t2} signal, it leads one to expect a damping, similar to that introduced by the $\Delta\omega_2$ signal. In fact this conjecture was substantiated by the performance of the sV_{t2} signal in the more complicated multimachine system representation.

The characteristic equation of the system with the Pa_2 stabilizer is determined by using equations (217), (218), and

$$\Delta V_{te} = K_6\Delta\phi_{fd} + K_5\Delta\delta - (Ds + Ms^2)K_a\Delta\delta \tag{2.28}$$

which in matrix form become

$$\begin{bmatrix} Ms^2 + Ds + K_1 & K_2 & 0 \\ K_4 & 1 + sT_{do} & \mu K_3 \\ K_a(Ds + Ms^2) - K_5 & -K_6 & 1 \end{bmatrix} \begin{bmatrix} \Delta\delta \\ \Delta\phi_{fd} \\ \Delta V_{te} \end{bmatrix} = 0 \tag{2.29}$$

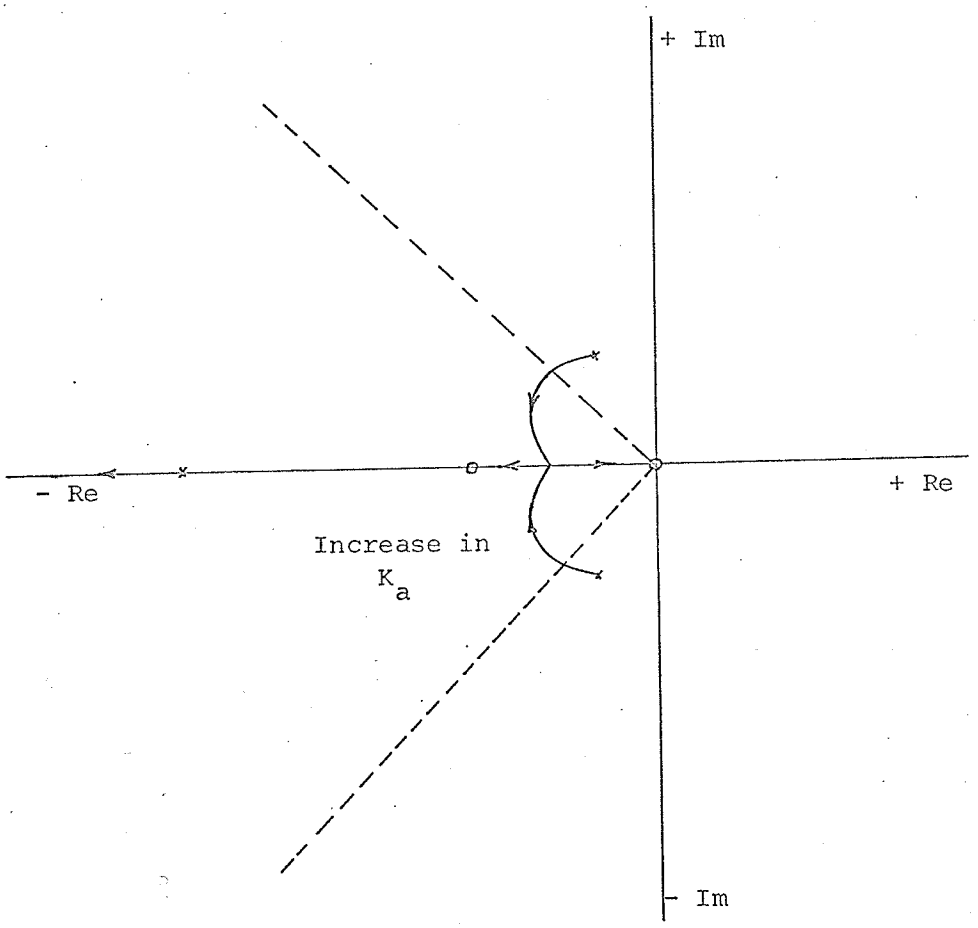

Figure 6. Root Locus with the P_{a2} Stabilizer Signal

with the characteristic equation

$$s^3 MT_{do} + s^2\{DT_{do} + M(1 + \mu K_3 K_6) + \mu M K_2 K_3 K_a\}$$
$$+ s^1\{K_1 T_{do} + D(1 + \mu K_3 K_6) + \mu D K_2 K_3 K_a\}$$
$$+ \{K_1(1 + \mu K_3 K_6) - K_2(K_4 + M K_3 K_5)\} = 0 \qquad (2.30)$$

The Pa_2 signal has modified the parametric root locus of the system by introducing an extra zero at

$$s = - D/M \qquad (2.31)$$

and the parametric root locus is of the form shown in Figure 6. It can be seen that by using an appropriate value of the gain K_a, the damping of the system can be increased and hence the stability can be improved. This was found to be true for the multi-machine model.

III. COMPLETE SYSTEM REPRESENTATION

Assumptions made in the model

1. The two machines represented are identical, i.e. they have the same ratings and machine constants. However, they have different excitation systems.

2. Ashern is considered to be replaced by a reactance and an infinite bus.

3. The voltages induced in the armature by the rate of change of armature flux linkages are negligible compared to the voltages generated by the fluxes rotating at fundamental speed.

4. Effects of amortisseur windings are not considered.

5. Armature and Transmission line resistances are neglected.

6. The mechanical power input remains constant during a disturbance. This is because the speeds of the generators do not change sufficiently to alter the governor setting and thence the gate position of the turbines during the short period for which the disturbance lasts.

7. Damping of the machines due to fundamental positive-sequence flux changes in the machines has been included. Excluded, however, is the damping due to:

(a) Interaction of the damper windings with any negative sequence fields,

(b) Interaction of damper windings with the field produced by any armature direct currents,

(c) Induction motor/generator action of the dampers and the positive sequence fields,

(d) Interaction of rotor circuits with the field produced by low frequency currents obtained as all machines swing slowly on the system, and

(e) Higher harmonic fields obtained with unbalanced operation or as a

consequence of abrupt system changes.

System Model, Block Diagram and Equations

The impedance diagram of the system is shown in Figure 7 and the phasor diagram of the system is shown in Figure 8. The sign convention being followed is that the d-axis component of the machine current is positive when it lags the q-axis component of the machine current by ninety electrical degrees, and is negative when it leads the q-axis component of the machine current by that amount.

Using this sign convention the system equations are as follows:

$$V_{qb1} = V_b \cos\delta_1 \tag{3.1}$$

$$V_{qb2} = V_b \cos\delta_2 \tag{3.2}$$

$$V_{db1} = V_b \sin\delta_1 \tag{3.3}$$

$$V_{db2} = V_b \sin\delta_2 \tag{3.4}$$

$$V_{qtb1} = V_{qb1} + x_{t2} I_{da1} \tag{3.5}$$

$$V_{qtb2} = V_{qb2} + x_{t2} I_{da2} \tag{3.6}$$

$$V_{dtb1} = V_{db1} - x_{t2} I_{qa1} \tag{3.7}$$

$$V_{dtb2} = V_{db2} - x_{t2} I_{qa2} \tag{3.8}$$

$$I_{da1} = I_{d1} + I_{d2} \cos(\delta_2 - \delta_1) \tag{3.9}$$

$$I_{da2} = I_{d1} \cos(\delta_2 - \delta_1) + I_{d2} \tag{3.10}$$

$$I_{qa1} = I_{q1} + I_{q2} \cos(\delta_2 - \delta_1) \tag{3.11}$$

$$I_{qa2} = I_{q1} \cos(\delta_2 - \delta_1) + I_{q2} \tag{3.12}$$

$$I_{d1} = (E_{i1} - V_{qtb1})/(x_{t1} + x_d) \tag{3.13}$$

$$I_{d2} = (E_{i2} - V_{qtb2})/(x_{t1} + x_d) \tag{3.14}$$

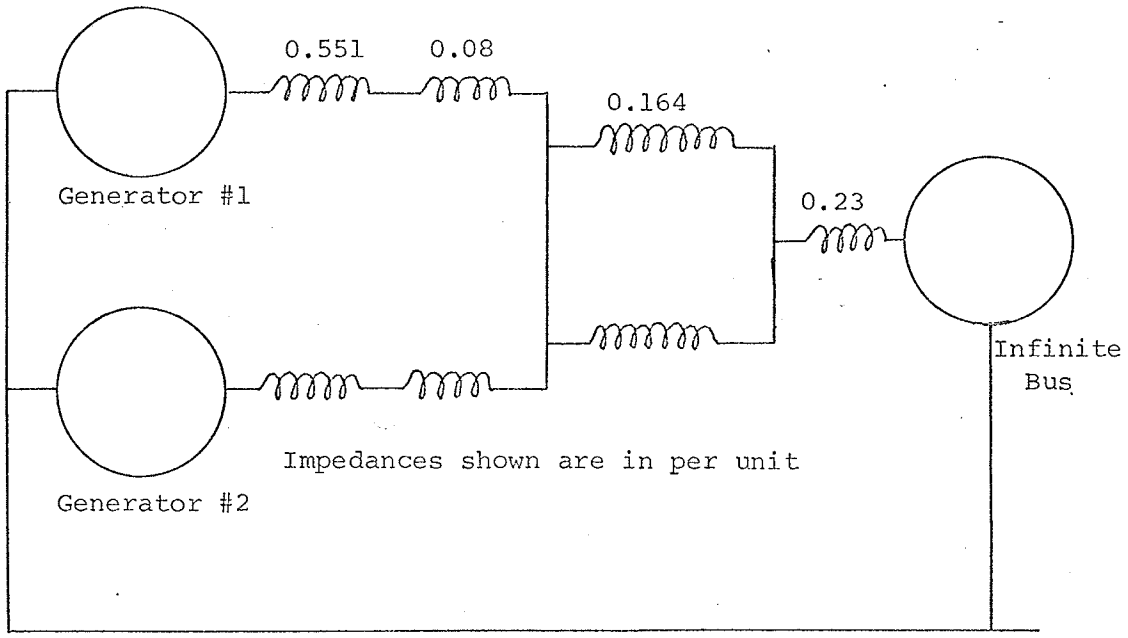

Figure 7. Impedance Diagram of the System

Table of Machine Constants

Maximum Output = 115 mw. per machine

Terminal Voltage = 13.8 kv.

x_d = .697 p.u.	T_{do}' = 5.10 sec.
x_q = .406 p.u.	T_{do}'' = 0.042 sec.
x_d' = .185 p.u.	T_{qo}'' = 0.089 sec.
x_q' = .406 p.u.	H = 5.65 mw-sec/mva
x_d'' = .142 p.u.	M = .03 mw-sec/mva-radian
x_q'' = .138 p.u.	

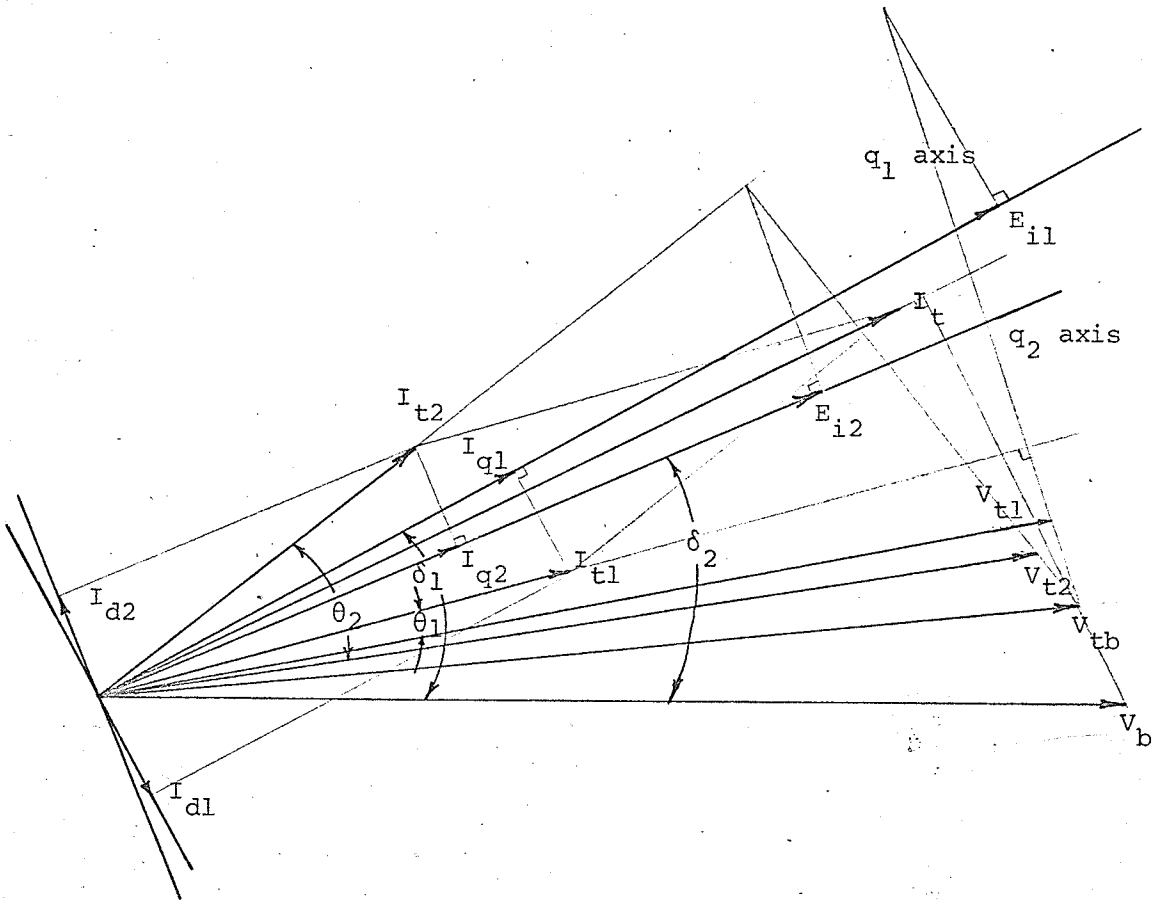

Figure 8. Phasor Diagram for the 3-machine System

$$I_{q1} = V_{dtb1}/(x_{t1} + x_q) \tag{3.15}$$

$$I_{q2} = V_{dtb2}/(x_{t1} + x_q) \tag{3.16}$$

The equations (3.9) through (3.16) are substituted in (3.5) through (3.8) to give

$$V_{qtb1} = V_{qb1} + x_{t2}\{E_{i1} - V_{qtb1} + (E_{i2} - V_{qtb})\cos(\delta_2 - \delta_1)\}/(x_{t1} + x_d) \tag{3.17}$$

$$V_{dtb1} = V_{db1} - x_{t2}\{V_{dtb1} + V_{dtb2}\cos(\delta_2 - \delta_1)\}/(x_{t1} + x_q) \tag{3.18}$$

$$V_{qtb2} = V_{qb2} + x_{t2}\{(E_{i1} - V_{qtb1})\cos(\delta_2 - \delta_1) + E_{i2} - V_{qtb2}\}/(x_{t1} + x_d) \tag{3.19}$$

$$V_{dtb2} = V_{db2} - x_{t2}[V_{dtb1}\{\cos(\delta_2 - \delta_1)\} + V_{dtb2}]/(x_{t1} + x_q) \tag{3.20}$$

The equations (3.17) to (3.18) are rewritten in the matrix form

$$\begin{bmatrix} x_{t1} + x_{t2} + x_d & x_{t2}\cos(\delta_2 - \delta_1) \\ x_{t2}\cos(\delta_2 - \delta_1) & x_{t1} + x_{t2} + x_d \end{bmatrix} \begin{bmatrix} V_{qtb1} \\ V_{qtb2} \end{bmatrix} = \begin{bmatrix} V_{qb1}(x_{t1} + x_d) + x_{t2}\{E_{i1} + E_{i2}\cos(\delta_2 - \delta_1)\} \\ V_{qb2}(x_{t1} + x_d) + x_{t2}\{E_{i1}\cos(\delta_2 - \delta_1) + E_{i2}\} \end{bmatrix} \tag{3.21}$$

$$\begin{bmatrix} x_{t1} + x_{t2} + x_q & x_{t2}\cos(\delta_2 - \delta_1) \\ x_{t2}\cos(\delta_2 - \delta_1) & x_{t1} + x_{t2} + x_q \end{bmatrix} \begin{bmatrix} V_{dtb1} \\ V_{dtb2} \end{bmatrix} = \begin{bmatrix} V_{db1}(x_{t1} + x_q) \\ V_{db2}(x_{t1} + x_q) \end{bmatrix} \tag{3.22}$$

The solutions of equations (3.21) and (3.22) represent a network solution for the system. As the system grows in size, i.e. there are more generators, the size of the matrices increases. When there are n generators feeding an infinite bus the coefficient matrix is of order $n \times n$.

The active and reactive power outputs of the system can be computed from the d- and q-axis components of the voltage and currents as follows:

$$V_{d1} = x_q I_{q1} \tag{3.23}$$

$$V_{q1} = V_{qtb1} + x_{t1} I_{d1} \tag{3.24}$$

$$V_{t1} = \sqrt{V_{d1}^2 + V_{q1}^2} \tag{3.25}$$

$$V_{d2} = x_q I_{q2} \tag{3.26}$$

$$V_{q2} = V_{qtb2} + x_{t1} I_{d2} \tag{3.27}$$

$$V_{t2} = \sqrt{V_{d2}^2 + V_{q2}^2} \tag{3.28}$$

$$P_{u1} = V_{d1} I_{d1} + V_{q1} I_{q1} \tag{3.29}$$

$$P_{u2} = V_{d2} I_{d2} + V_{q2} I_{q2} \tag{3.30}$$

$$Q_{u1} = V_{q1} I_{d1} - V_{d1} I_{q1} \tag{3.31}$$

$$Q_{u2} = V_{q2} I_{d2} - V_{d2} I_{q2} \tag{3.32}$$

$$P_u = P_{u1} + P_{u2} \tag{3.33}$$

$$Q_u = Q_{u1} + Q_{u2} \tag{3.34}$$

The power input to the system is assumed to be kept constant. The accelerating power is applied to the rotors of the two machines

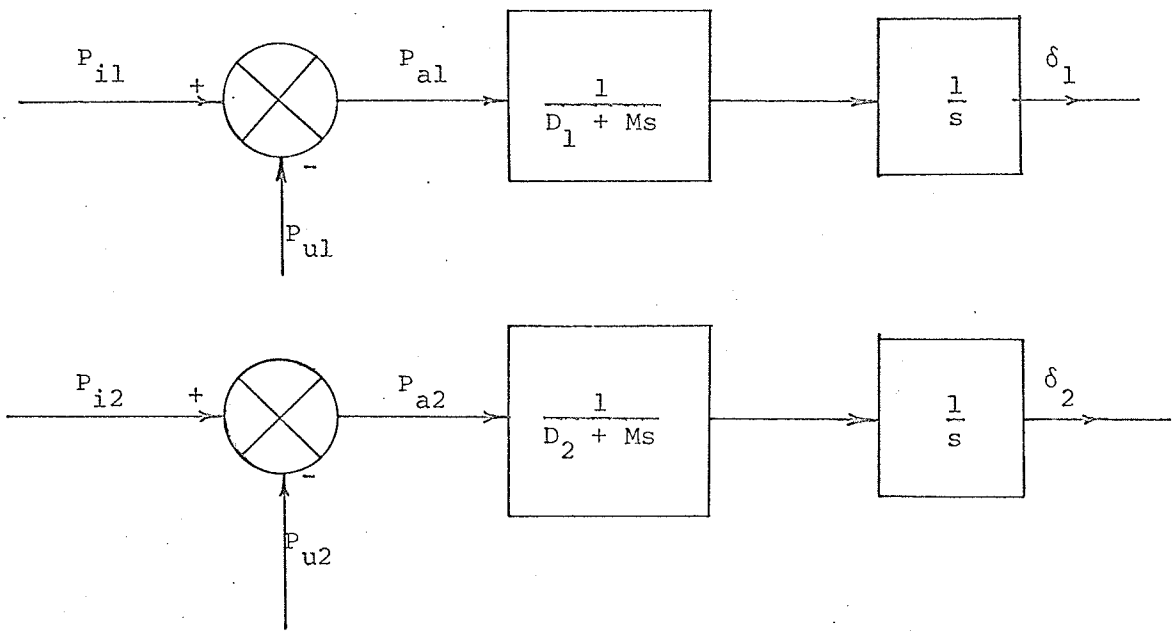

where M is the inertia constant of each machine and D_1 and D_2 the damping factors [17] of machines 1 and 2, respectively, are given by:

$$D_1 = T_{do}''(x_d' - x_d'')(V_b \sin\delta_1)^2/(x_d' + x_{t1} + x_{t2})^2 + T_{qo}''(x_q' - x_q'')(V_b \cos\delta_1)^2/(x_q' + x_{t1} + x_{t2})^2 \quad (3.35)$$

$$D_2 = T_{do}''(x_d' - x_d'')(V_b \sin\delta_2)^2/(x_d' + x_{t1} + x_{t2})^2 + T_{qo}''(x_q' - x_q'')(V_b \cos\delta_2)^2/(x_q' + x_{t1} + x_{t2})^2 \quad (3.36)$$

As the machines swing on the system, the positive-sequence field in the air gap interacts with the damper windings to produce a synchronizing torque. This torque is not negligible and changes with the electrical angles δ_1 and δ_2 of the two machines. Normally, this change is neglected and the damping factors are taken as constants. However, in this study the variations are taken into account and this results in a more accurate representation of the inherent damping of the machines. A certain amount of natural damping is also present due to the retarding influence of the field time constant on the armature reaction [13].

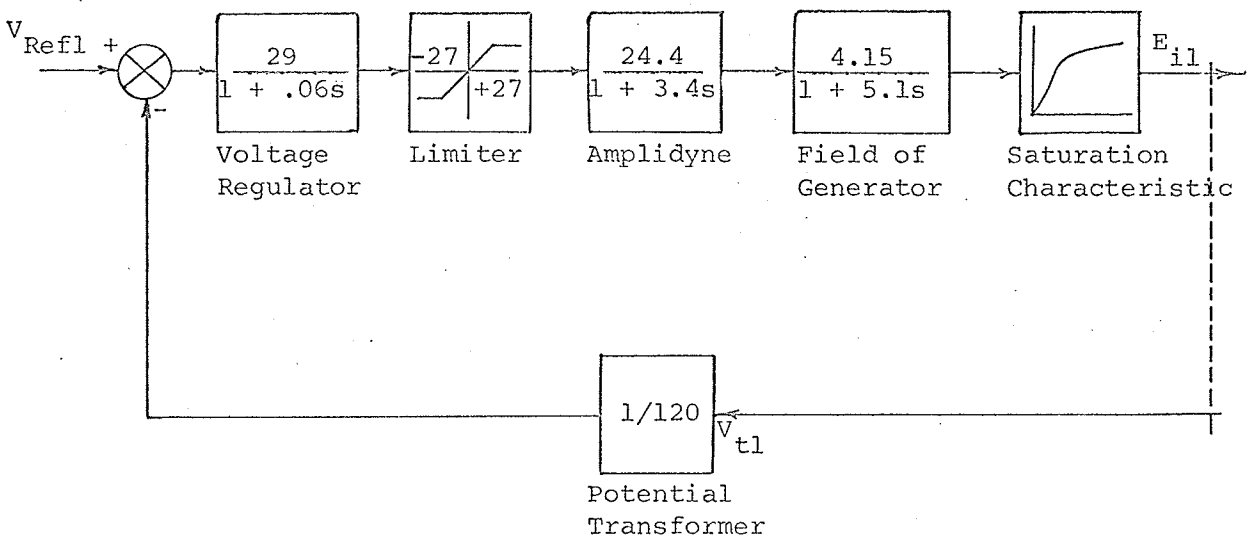

Figure 9. Excitation System of Machine 1

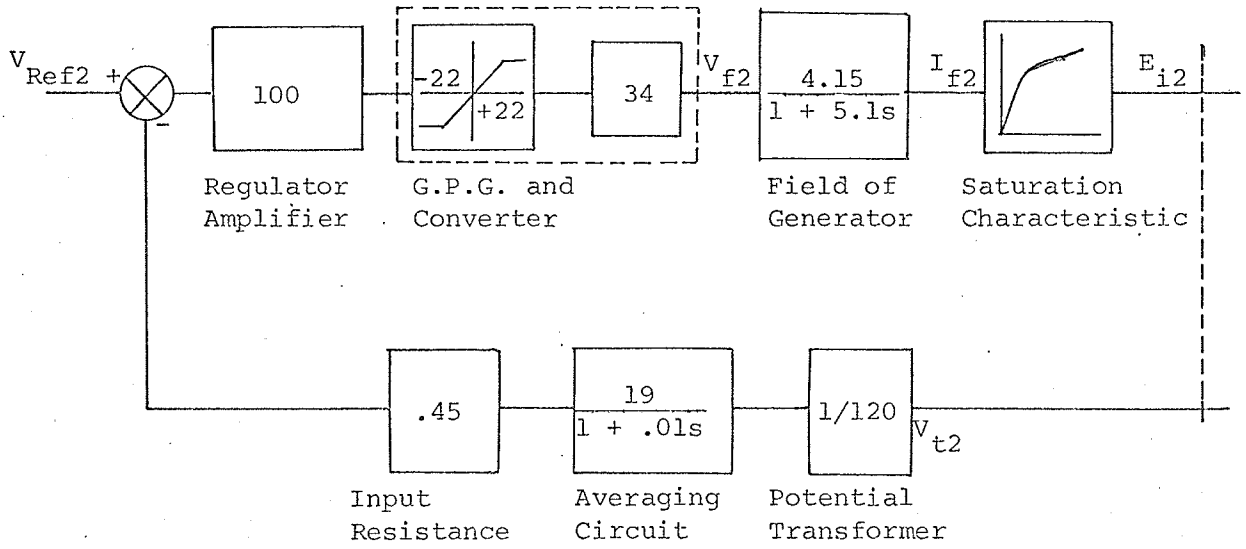

Figure 10. Excitation System of Machine 2

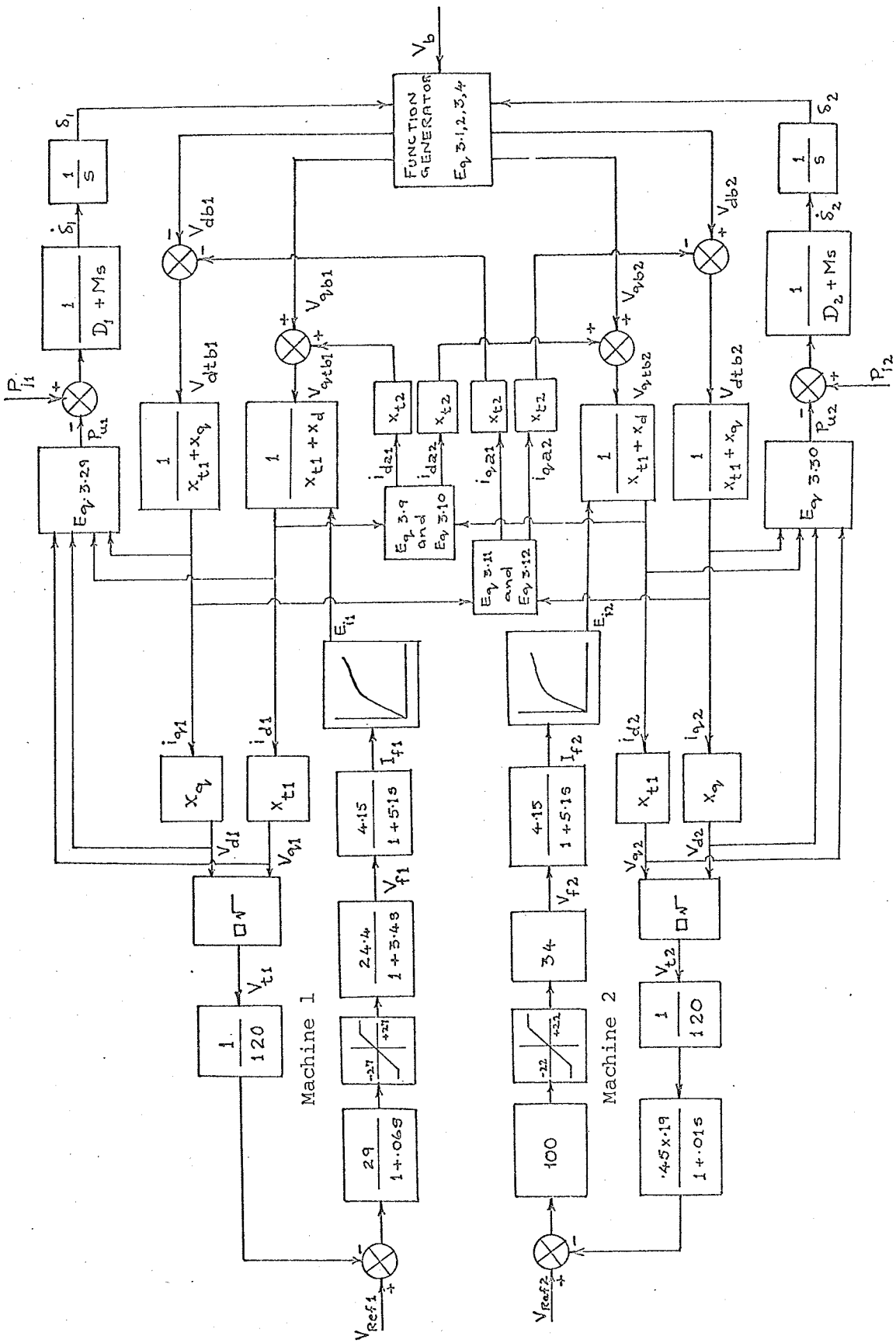

Figure 11. Block Diagram Representation of the 3-machine System

The excitation systems for the two machines are shown in Figures 9 and 10. A complete block diagram of the three machine system is shown in Figure 11.

The system model used has been adapted to include both direct and quadrature axis effects. The nonlinear saturation characteristic of the generators can be included as a further refinement of the model. The power factor angle is taken into account in the simulation study.

The model used considers the dynamic interaction between the two generators. This is of particular interest since one of the generators has conventional amplidyne excitation and the other has static excitation.

This model is a more adequate representation than the Heffron and Phillips model, [14], which is based on small oscillation theory. It may be argued that, for dynamic stability, a small region about the steady state should be considered and so justify the linearization about the steady state. However, it was found during the simulation with the above model that the field voltage of the machine with static excitation was initially driven to the peak value which was imposed by the limiter, and, since the peak swings do occur in the first few instants of the disturbance, it is therefore not reasonable to ignore the presence of the limiter for dynamic stability. Another difficulty in using the model based on the small oscillation theory is that it is quite arbitrary in setting the initial conditions for a simulation run [1].

IV. COMPUTATION AND RESULTS

Introduction

At first an attempt was made to model the system on the TR-48* analog computer. The equations of the system had to be scaled both in magnitude and time. It was found difficult to set up the nonlinearities. Another problem arose due to the limitation in the number of amplifiers, and it was soon realized that the TR-48 would be inadequate to handle the modelling of the 3-machine system. For the above reasons, the attempt to model the system on the analog computer, was abandoned.

A digital computer program called Continuous-System-Modelling-Program (CSMP) had been added to the IBM-360/65† computer library at the University and this enabled a block diagram approach to be made for modelling the system. By using the digital computer it was possible to use quantities like volts and megawatts instead of having to convert to per unit quantities. By suitably manipulating the block diagram a reasonable representation of the actual system was obtained. The CSMP program used is given in Appendix C.

First Test Series

A test run was made for a loading of 90 Mw (78% of full load) per machine. The variations of the electrical angle of each machine were obtained. For the dynamic stability test the time variations of the electrical angles of the machines for a 3.5% change in the reference voltage of machine 2 are shown in Figures 12 and 13, and for a -3.5%

---

*Trade-name for an Electronic Associates Inc. computer.

†International Business Machines Corporation designation.

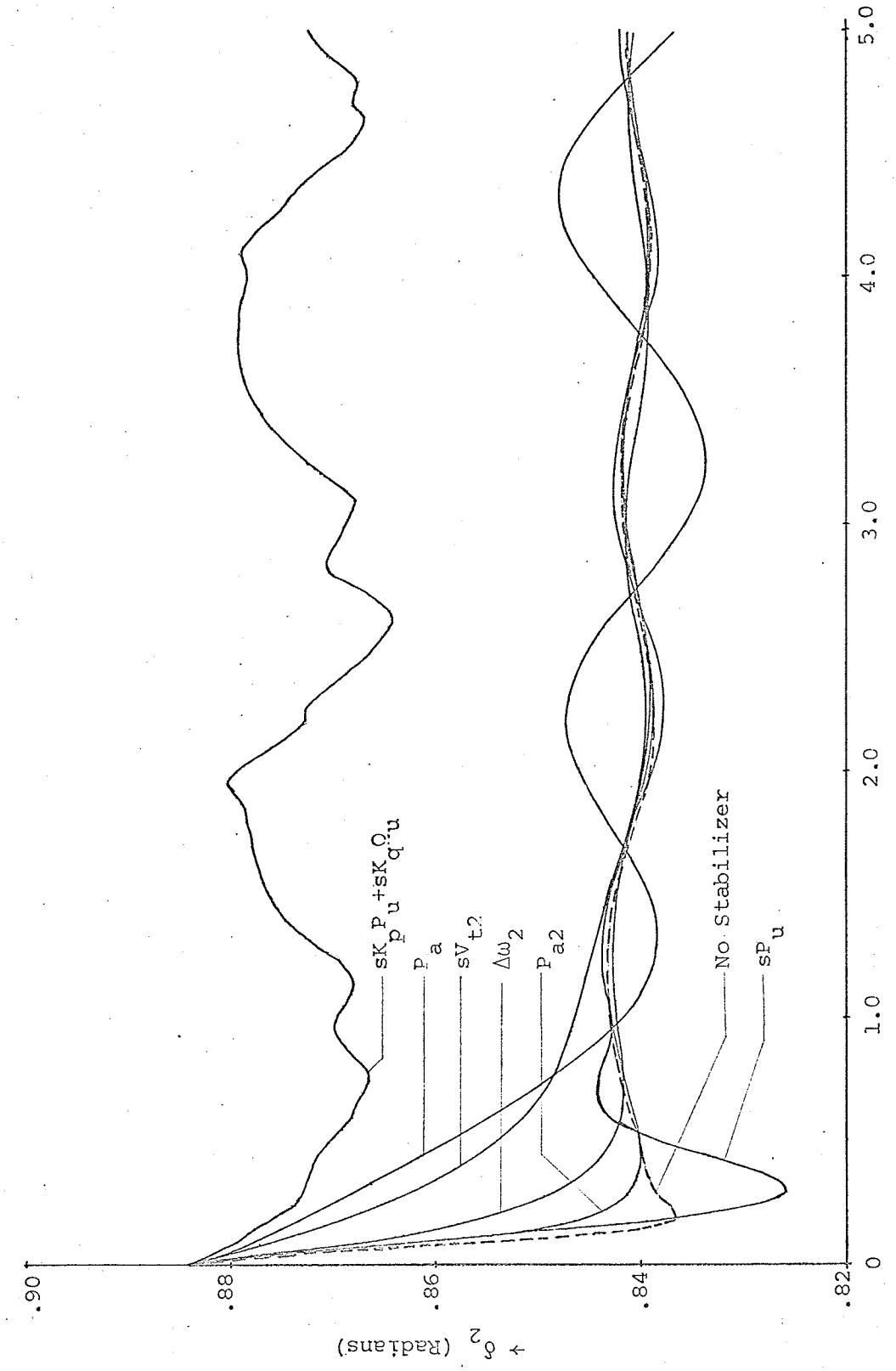

Figure 12. Dynamic Stability, 3.5%, 180 mw Load, $\dot{\delta}_2$ vs Time

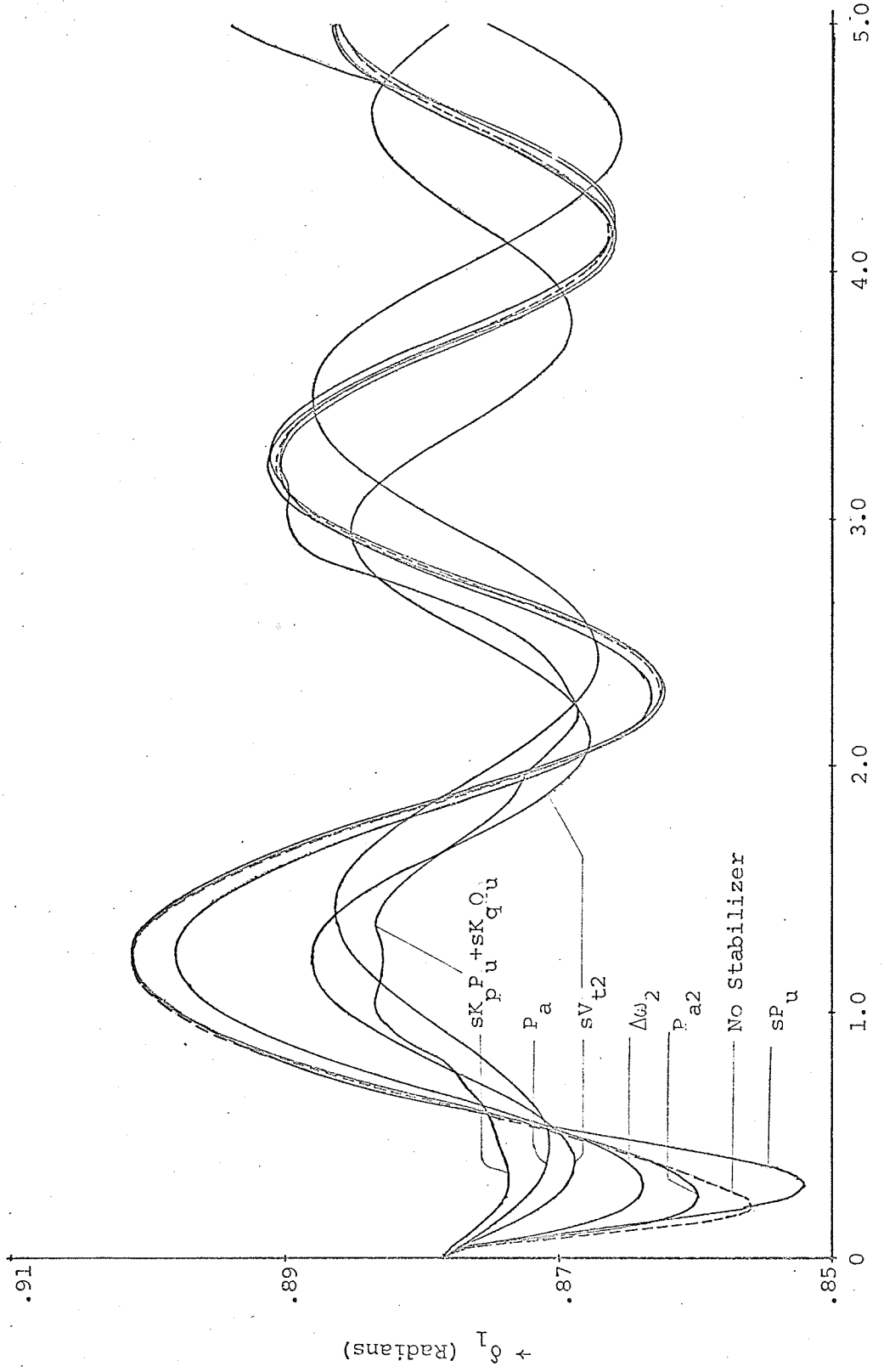

Figure 13. Dynamic Stability, +3.5%, 180 mw Load, δ_1 vs Time

change in the reference voltage of machine 2 is shown in Figures 14 and 15. The variations of the electrical angles of the machines during the Transient Stability test are shown in Figures 16 and 17.

It is seen that although the stabilizer signals were applied to the field of machine 2 only, i.e. the machine with static excitation, they also had an effect on the oscillations of machine 1, i.e. the machine with conventional amplidyne excitation.

The speed error signal, $\Delta\omega_2$, was reasonably satisfactory in improving the system performance. However, to get a "clean" $\Delta\omega_2$ signal in practice can be difficult. The complications involved have been discussed [10] and it is pointed out that the speed error signal must be extremely sensitive to small variations in the speed. A number of signal processing circuits have to be introduced, as well as a complicated gear wheel mechanism [10].

In this study the recorded transients indicate that the effect of the $\Delta\omega_2$ signal is very closely approximated by the signal which is the derivative of the terminal voltage (sV_{t2}), and to the signal which is proportional to the accelerating power (P_{a2}), of machine 2. These last two signals should be more suitable to use in practice because to obtain them does not require complex mechanical parts as are necessary for obtaining the $\Delta\omega_2$ signal.

The effect of other signals such as the derivative of active power (sP_u), derivative of the sum of reactive and active power ($sK_pP_u + sK_qQ_u$), and a signal proportional to the system accelerating power have also been shown. It can easily be seen from the graphs that none of these signals is suitable. Although for dynamic stability (+3.5%) the $sK_pP_u + sK_qQ_u$ signal initially provides maximum damping for machine 1, the oscillations

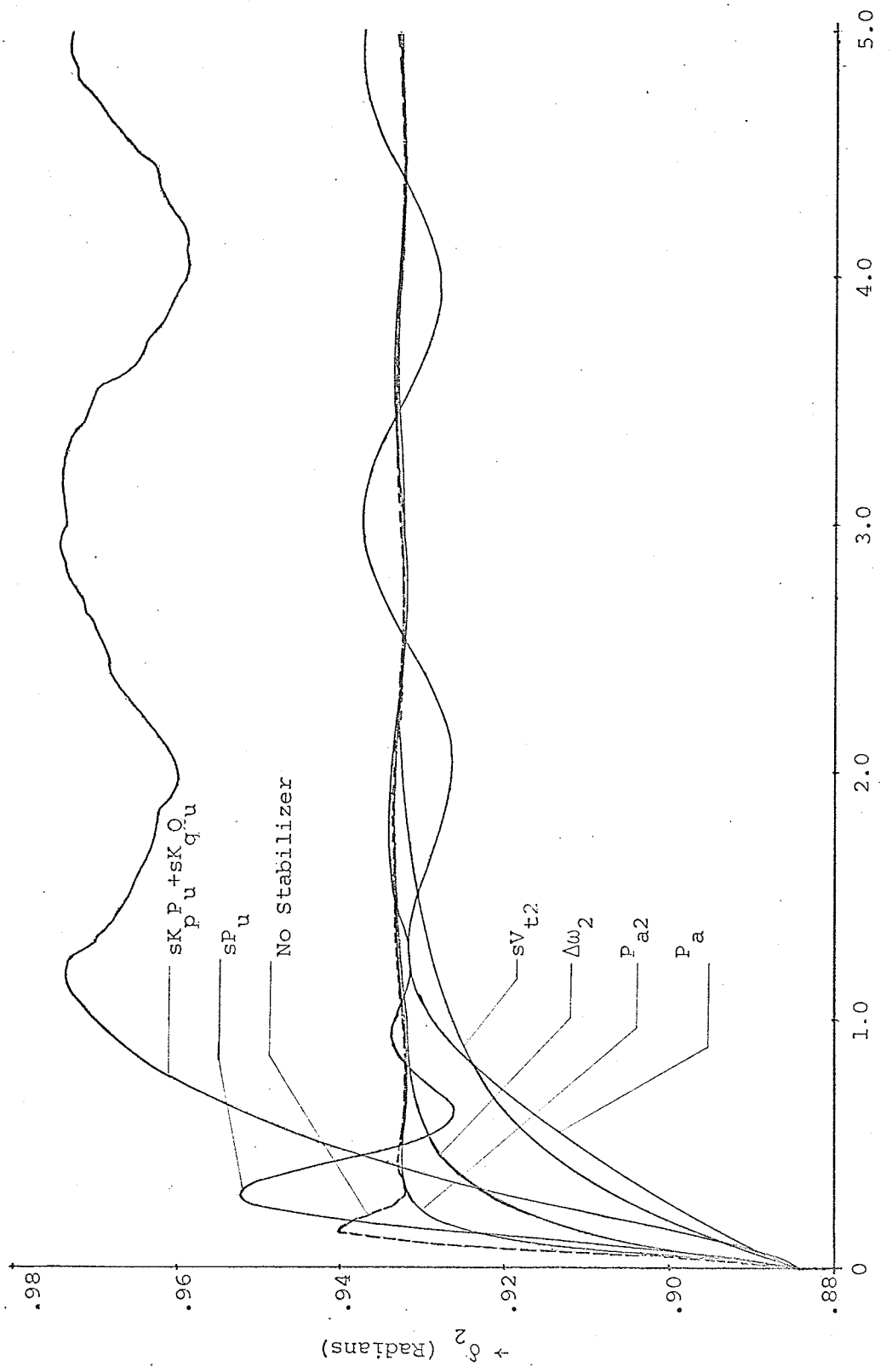

Figure 14. Dynamic Stability -3.5%, 180 mw Load, δ_2 vs Time

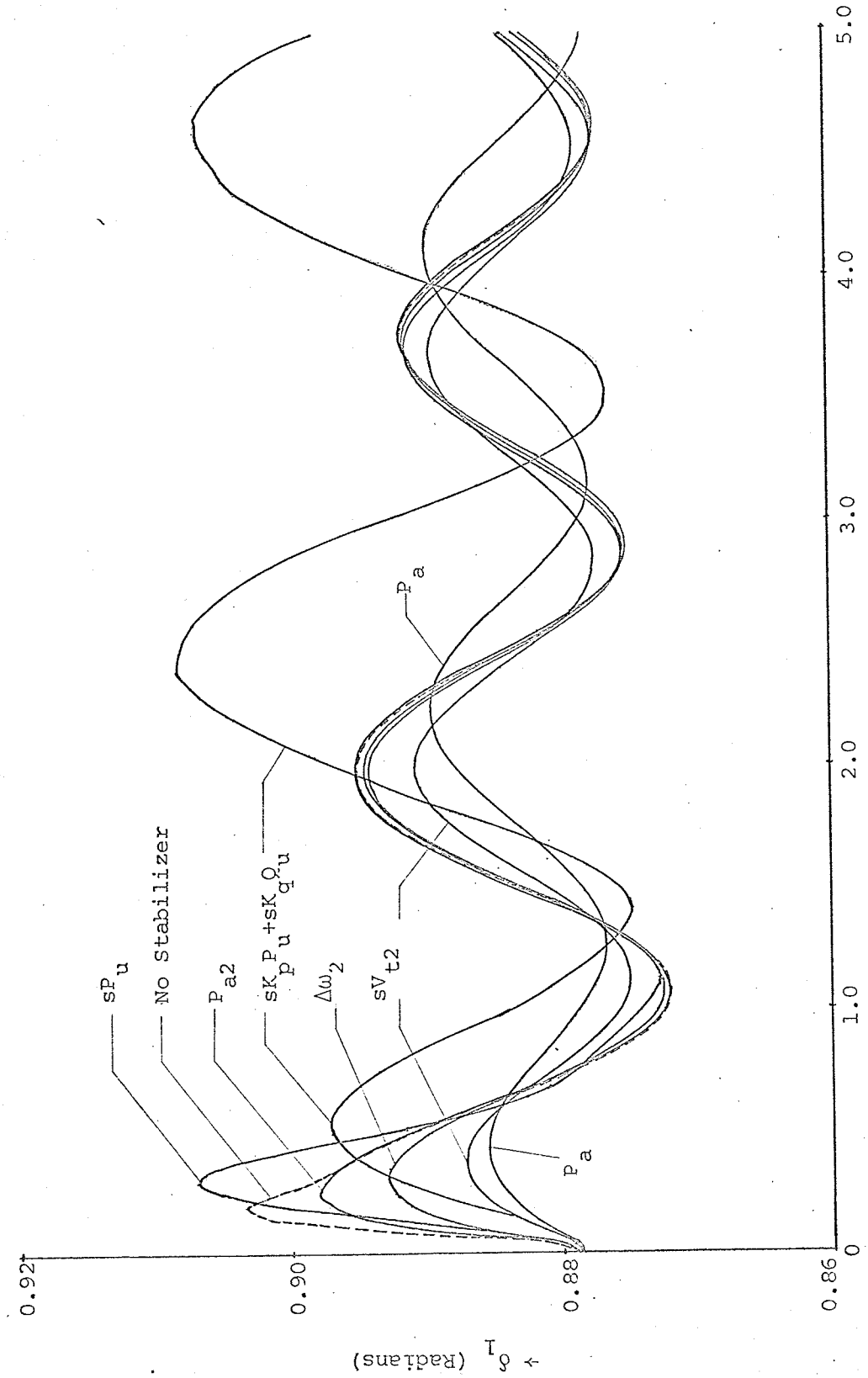

Figure 15. Dynamic Stability, -3.5%, 180 mw Load, δ_1 vs Time

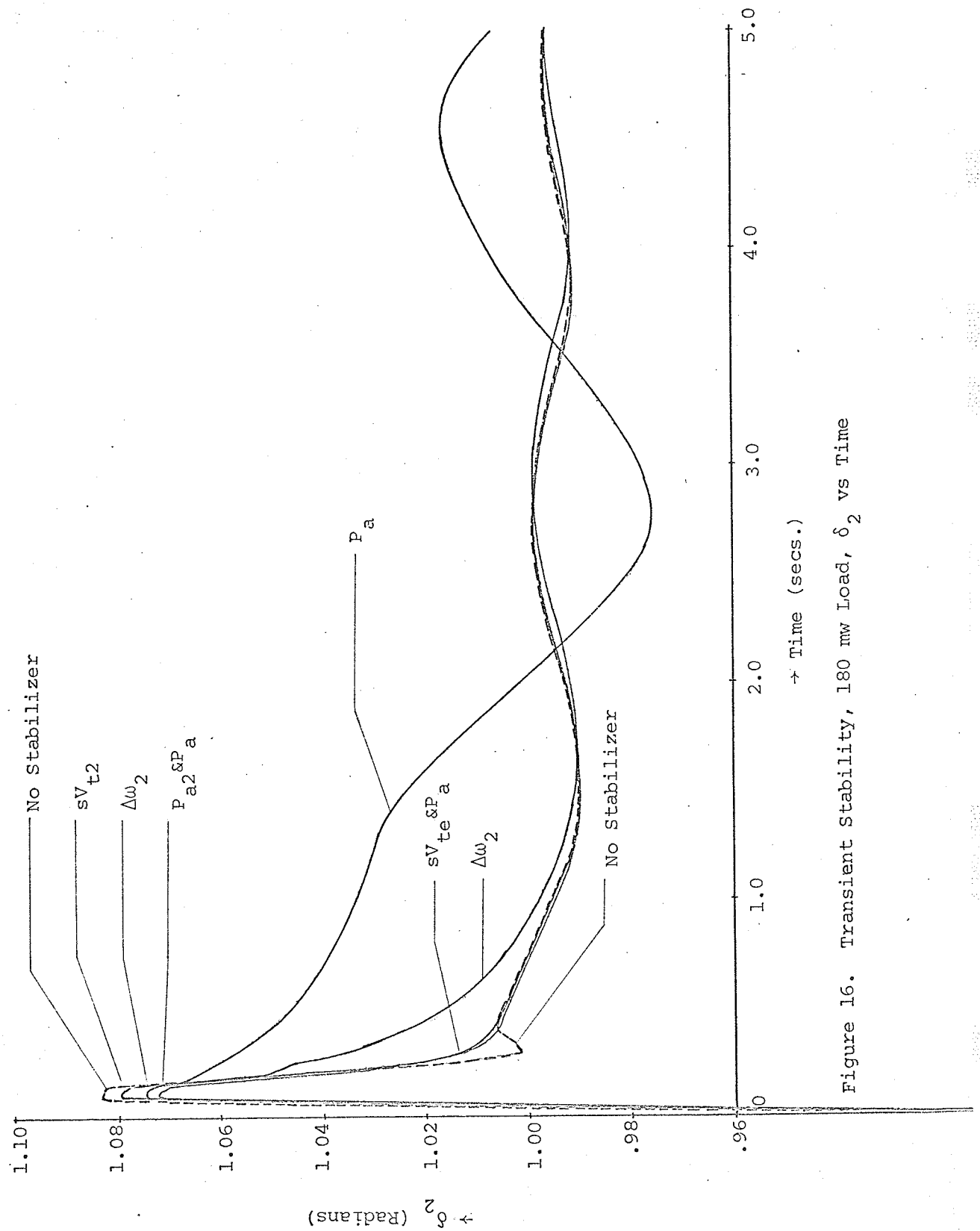

Figure 16. Transient Stability, 180 mw Load, δ_2 vs Time

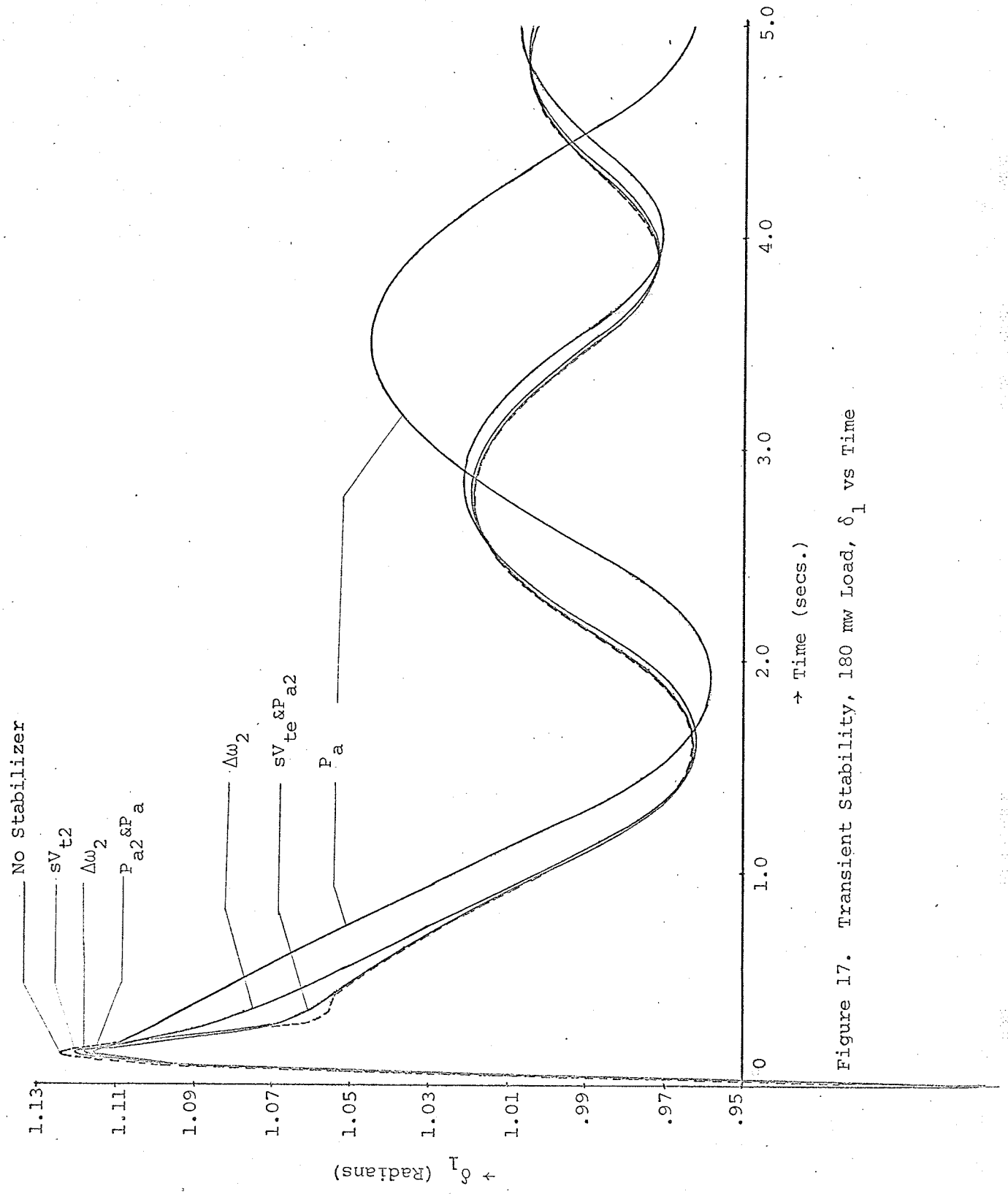

Figure 17. Transient Stability, 180 mw Load, δ_1 vs Time

begin to grow; in addition, the behaviour of machine 2 becomes highly oscillatory. When the $sK_pP_u + sK_qQ_u$ signal is used for improving the transient stability, machine 2 is forced to slip a pole. The trace for this is not shown in the Figures. The signal proportional to sP_u made both machine 1 and machine 2 more oscillatory for both dynamic and transient stabilities. The signal proportional to the system accelerating power is able to provide a large amount of damping initially but after that it accentuates the build up of oscillations and so has to be classified as unsatisfactory.

It is interesting to note that the signal proportional to the accelerating power of machine 2 tends to stabilize not only machine 2 but machine 1 as well. However, a signal proportional to the system accelerating power cannot stabilize the system. This is probably due to the fact that machine 1 has a larger time constant in the feedback system and is unable to respond quickly enough. Thus machine 2 gets a disproportionately large corrective signal due to the slow fluctuation of the power output of machine 1. However, when the feedback is from the accelerating power of machine 2 to the field of machine 2 itself, then it is not directly subjected to disturbances such as the slow power fluctuations of machine 1. Incidentally, the effect of this signal vividly illustrates the interactions between the two machines.

Second Test Series

After the first set of tests it was decided to impose more severe loadings on the machines. By trial and error, a loading was found such that the responses of the machines were highly oscillatory before the stabilizer signals were applied.

For transient stability a suitable loading was found to be 94.2 mw

(82% of full load) on each machine. When one transmission line is switched out, machine 1 slips a pole and consequently causes machine 2 to oscillate violently during the time it is slipping. The $s\Delta_{t2}$, $\Delta\omega_2$, and P_{a2} signals were almost equally effective in damping machine 2 and in stabilizing the system by preventing machine 1 from slipping the pole. The effect of each of the stabilizer signals on the electrical angles of the machines is illustrated in Figures 18 and 19.

From the first test, it was also realized that the criterion used by Manitoba Hydro to determine the response of their system, in so far as dynamic stability is concerned, is only an approximate one and in effect the 3.5% change in the reference voltage of machine 2 that they use for testing is too much. The system is forced into the nonlinear region and this contradicts the definition of dynamic stability which assumes that the system is working in a linear region. For the above reason, it was decided to test the model for dynamic stability with a 1% change in the reference voltage of machine 2. To make the system more oscillatory the tests were made with loadings of 117.5 mw (102% of full load) per machine. This time again it was found that the $\Delta\omega_2$, sV_{t2}, and P_{a2} stabilizer signals improved the damping and hence the dynamic stability of the system. The variations in the electrical angles of the machines are shown in Figures 20 and 21. The total power rate, sP_u, signal was tried again since its effect had been predicted to be good by the small oscillation theory. However, in spite of the optimizing of the magnitude of the total power rate signal it did not provide any significant damping.

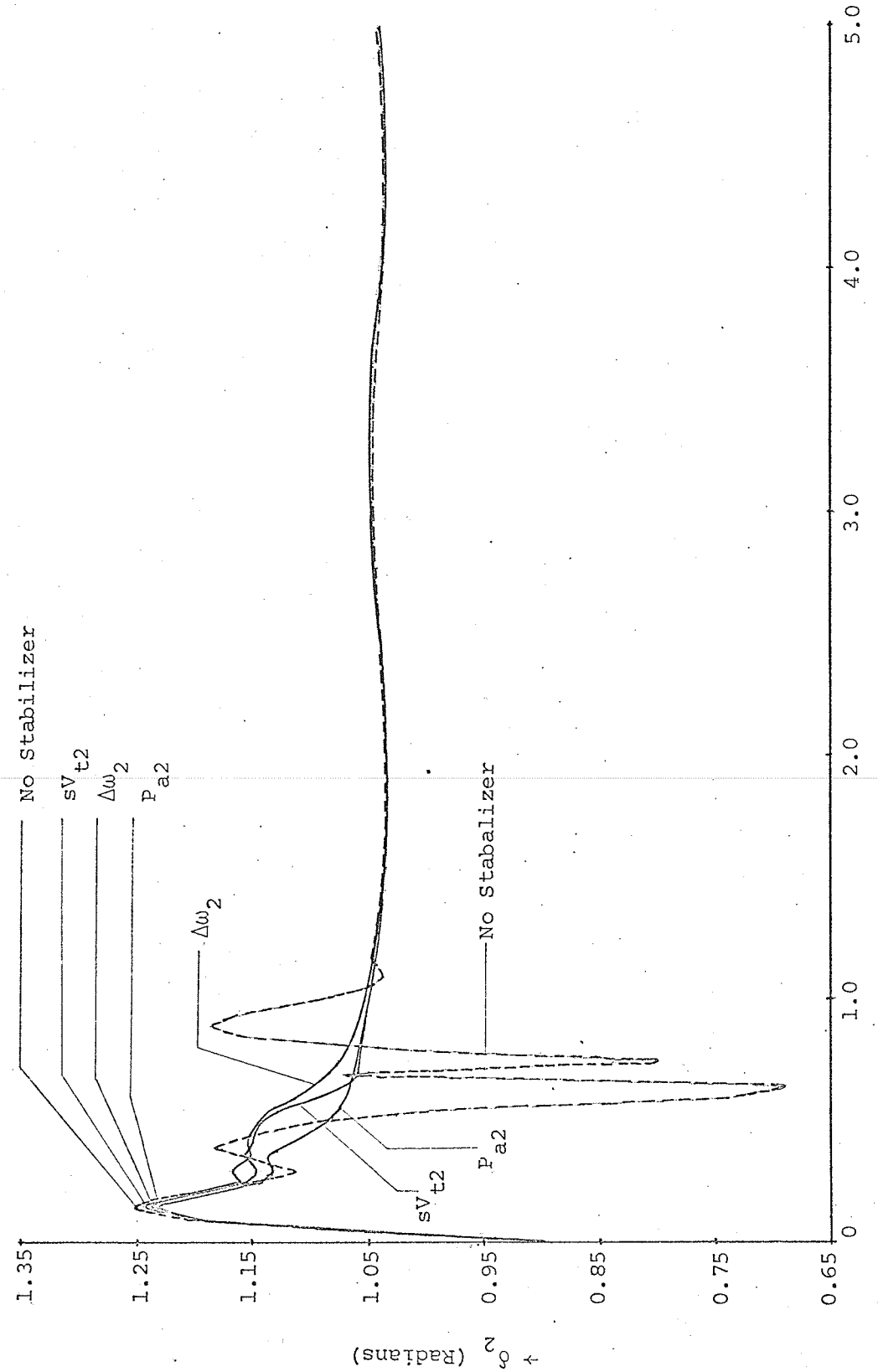

Figure 18. Transient Stability, 188.4 mw Load, δ_2 vs Time

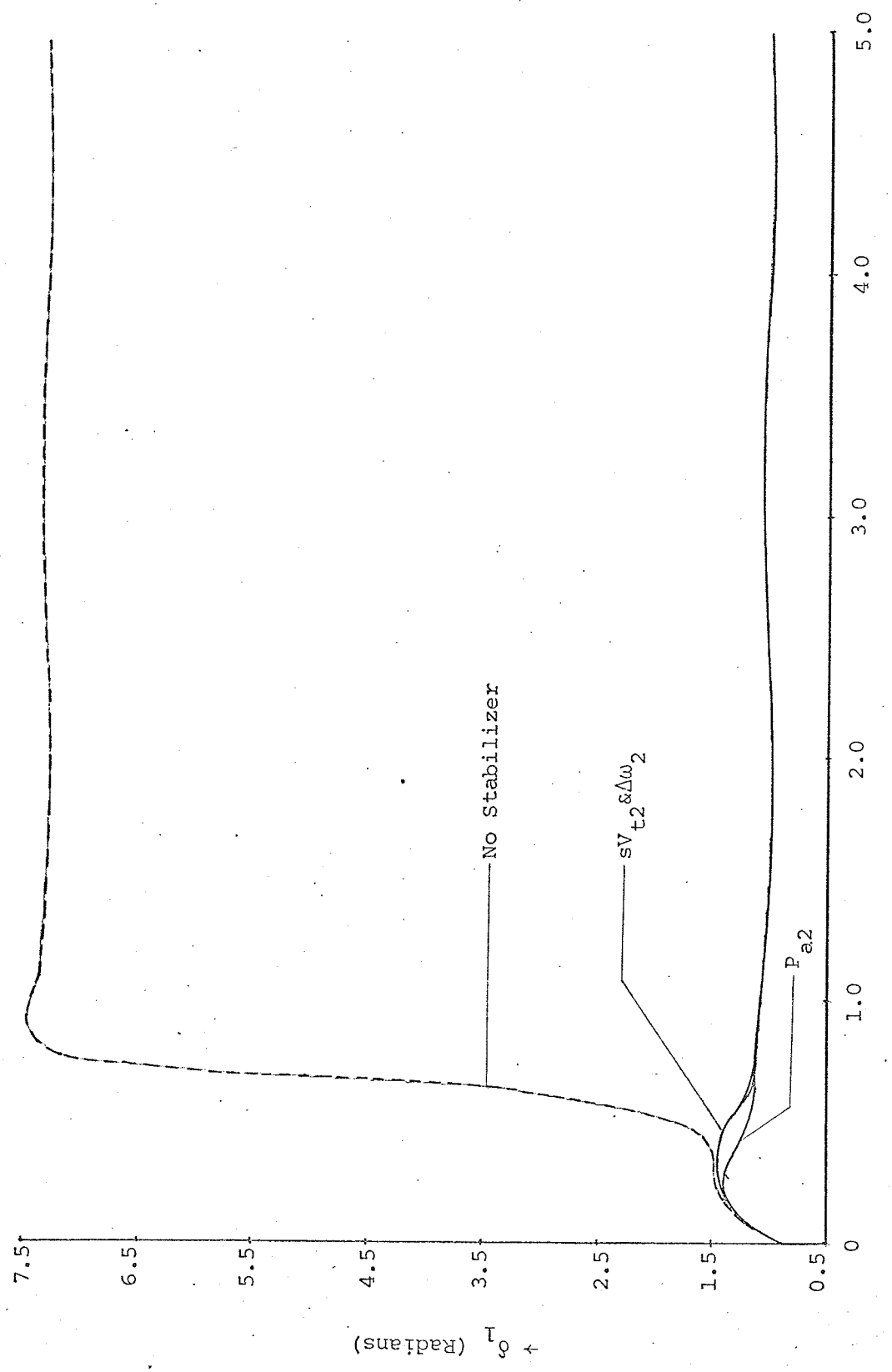

Figure 19. Dynamic Stability, -1%, 235 mw Load, δ_1 vs Time

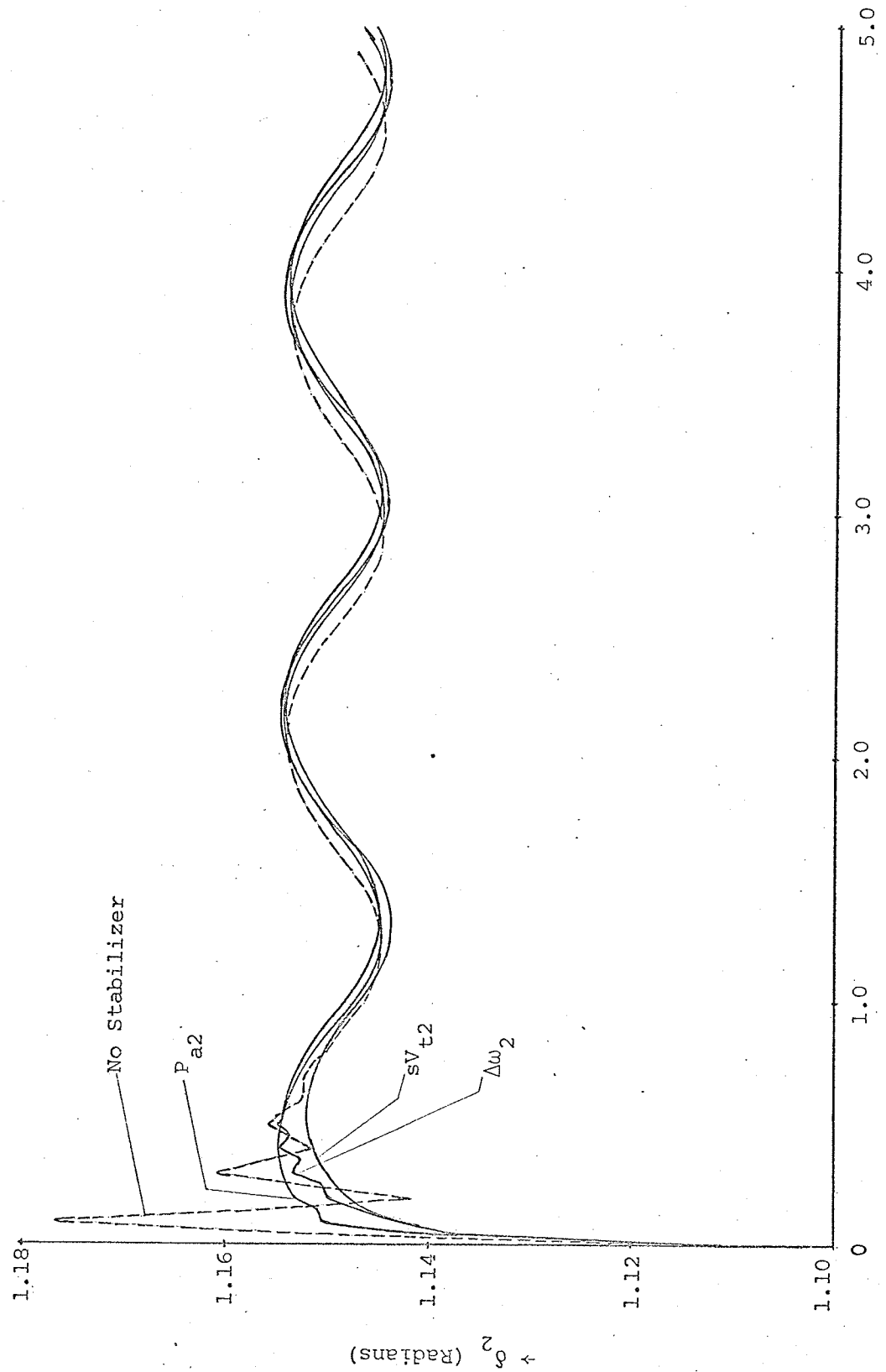

Figure 20. Dynamic Stability, -1%, 235 mw Load, δ_2 vs Time

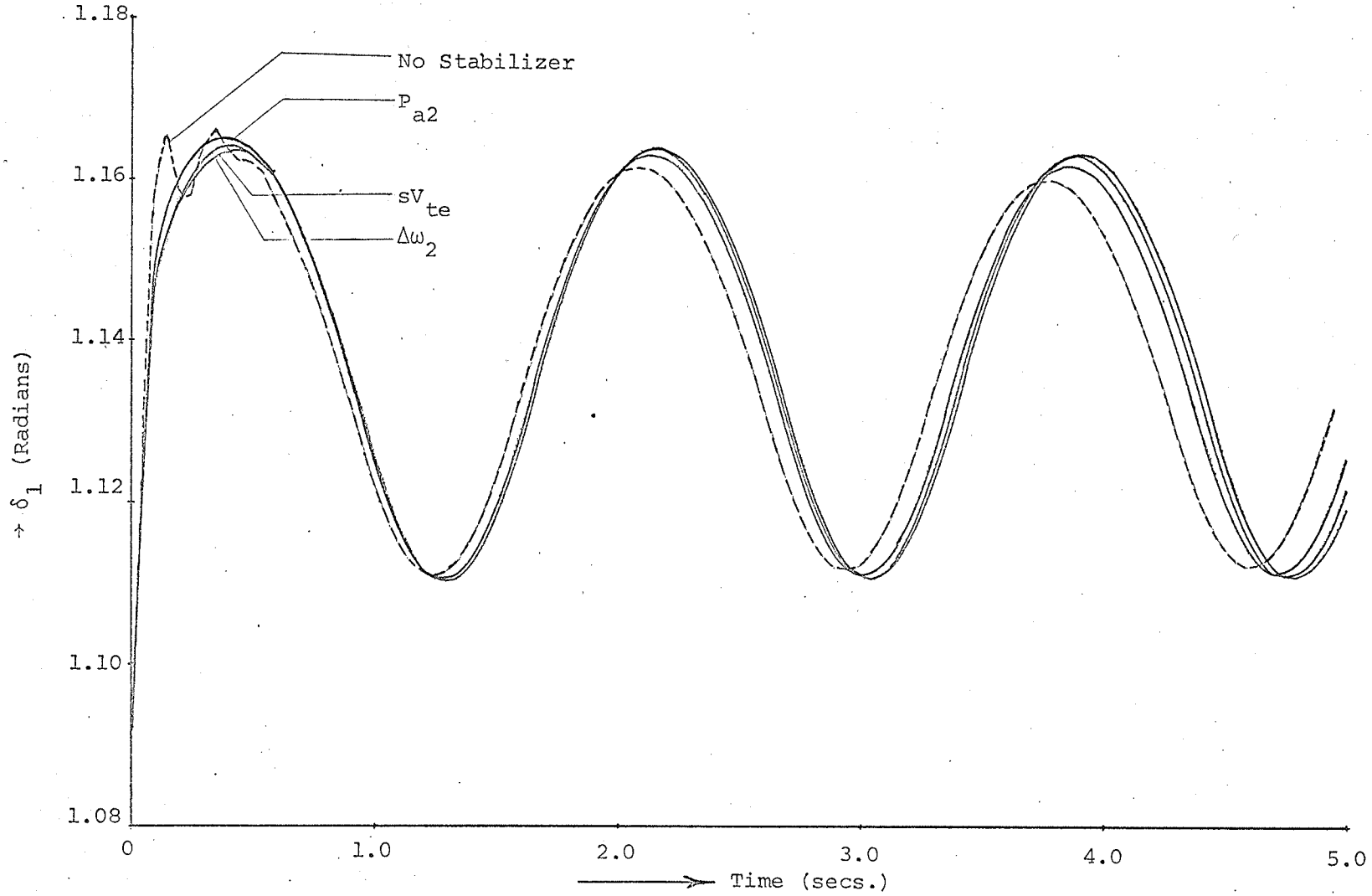

Figure 21. Dynamic Stability, -1%, 235 mw Load, δ_1 vs Time

V. GENERAL CONCLUSIONS

From the simulations of the model, it can be concluded that the $\Delta\omega_2$, sV_{t2}, and P_{a2} stabilizer signals could improve the dynamic and transient stabilities of the system to about the same degree.

This being a problem of practical nature, one must determine whether or not such signals can be obtained in practice. The $\Delta\omega_2$ signal can be obtained by using the complicated mechanical arrangement suggested by Dandeno et al. [10]. A similar arrangement was tested by Manitoba Hydro on their machine at Grand Rapids and found to be satisfactory. An sV_{t2} signal can also be obtained; a suitable technique is described in Appendix A. A technique for obtaining a P_{a2} signal is discussed in Appendix B.

Comparing the effect of the $\Delta\omega_2$, sV_{t2}, and P_{a2} signals, one would prefer to use either the sV_{t2} or the P_{a2} stabilizer signal because they are relatively easy to obtain. In choosing between the sV_{t2} and the P_{a2} signals one would prefer to use the P_{a2} stabilizer signal since it requires fairly simple electrical circuit implementation circuitry.

Interlocks should be provided so that when the operator tries to vary the voltage or power intentionly, the stabilizer signals are cut out. Also if the circuit breakers trip the interlocks should automatically cut out the stabilizer signal.

The model discussed could also be used to simulate the runs for unequal loadings of the machines. This would be of practical significance since the machines are not necessarily run at equal loads.

The model used is essentially a single-phase equivalent model of the system and thus is valid only for symmetrical faults or switching. However, in practice, one anticipates what to expect in any sort of contingency. To that end one should have a more general 3-phase

representation which would take into account the asymetrical faults and asymetrical loading of the transmission lines. Stability analysis should incorporate a means for the determination of the fault currents, etc., in each of the phases because the severity of the fault will determine the subsequent transients. As soon as the fault is removed the transient or residual fluxes left behind will influence the initial conditions from which the stabilizers have to operate in order to keep the machines in synchronism. Thus a 3-phase model should be developed by which various initial conditions could be established into each of the phases.

A. TECHNIQUE FOR OBTAINING THE VOLTAGE DERIVATIVE SIGNAL

The sV_{t2} signal is obtained by taking the derivative of the V_{t2} signal which is obtained at the output of the 3-phase rectifier bridge.

The rectified voltage has a high frequency ripple as is shown in Figure 22b, the derivative of which will contain a series of undesirable pulses. In order that the output signal be zero when such high frequency differentiated the proposed circuit arrangement shown in Figure 23a is used. Now when there is a variation in the system, the envelope of the terminal voltage will vary in magnitude. The effect will be as if the terminal voltage acted as a carrier wave with the low frequency modulation representing the variations on the system, as shown in Figure 22a.

The input-output relationship for the operational circuit arrangement is $E_o/E_{in} = - [j\omega R_2 C_1/\{(1 + j\omega R_1 C_1)(1 + j\omega R_2 C_2)\}]$ the Bode plot for which is shown in Figure 23b for the case where in $R_1 C_1 = R_2 C_2 \equiv 1/\omega_o$. The frequency ω_o can be adjusted in such a way that the high frequency noise, which in this case includes the high frequency ripple, is attenuated. Then we should be able to get a smooth sV_{t2} signal, as shown in Figure 22c, as long as the significant frequencies of V_{t2} are well below ω_o rad./sec.

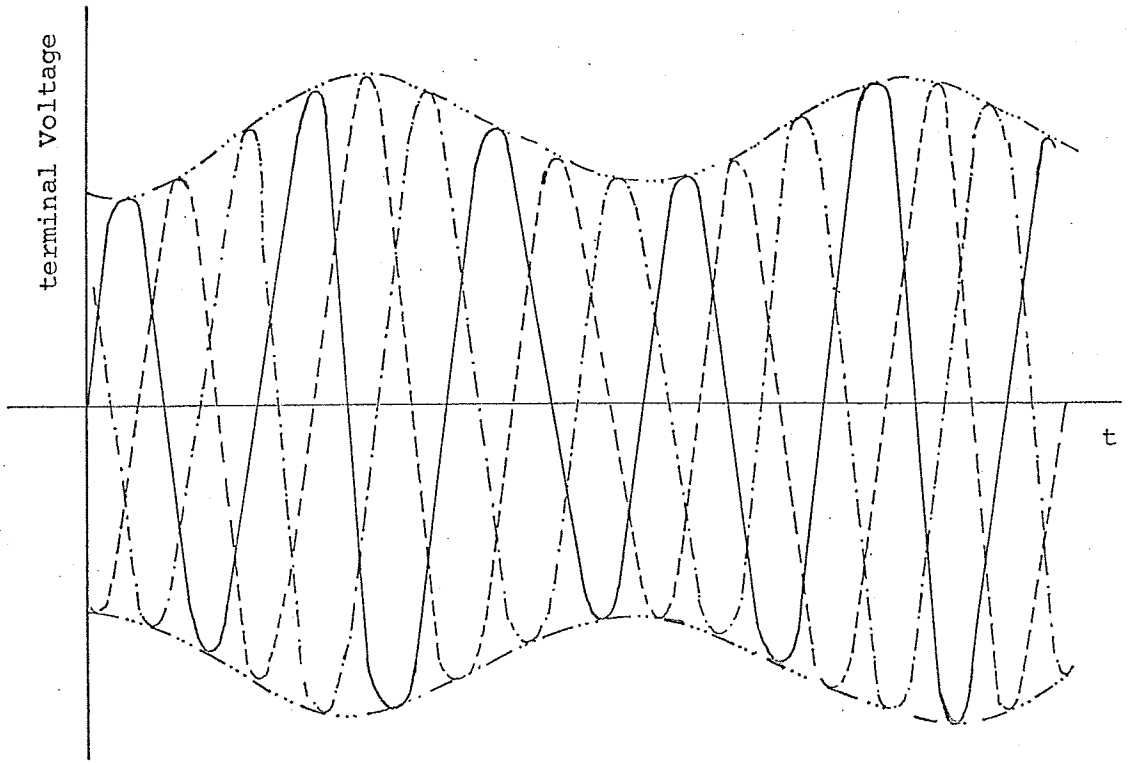

Figure 22a. Variation in the terminal Voltage

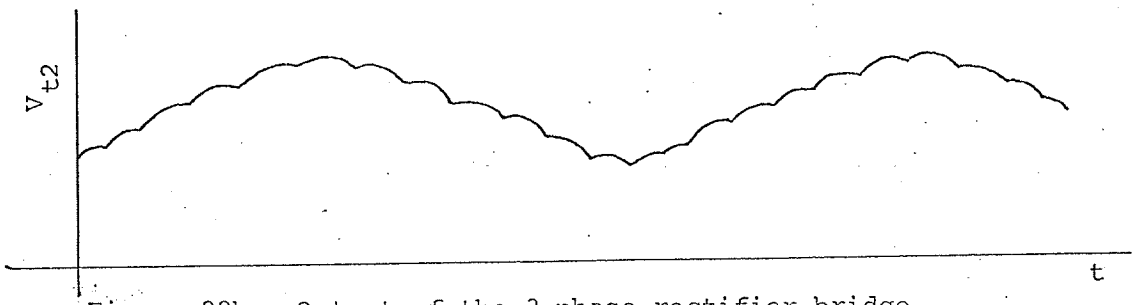

Figure 22b. Output of the 3-phase rectifier bridge

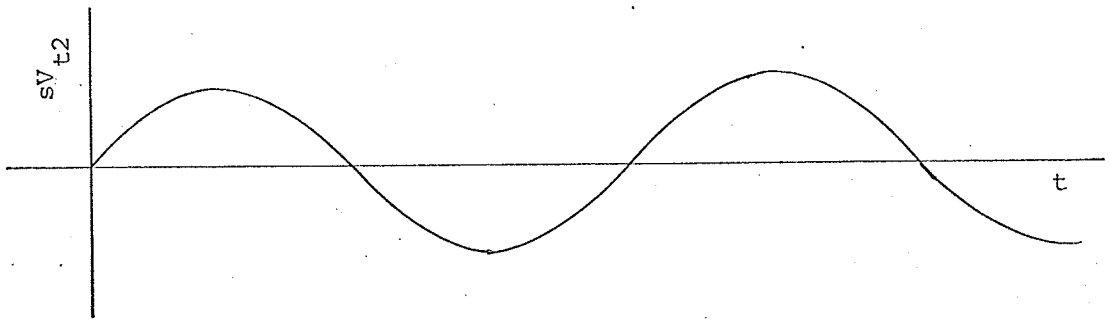

Figure 22c. Voltage derivative Signal

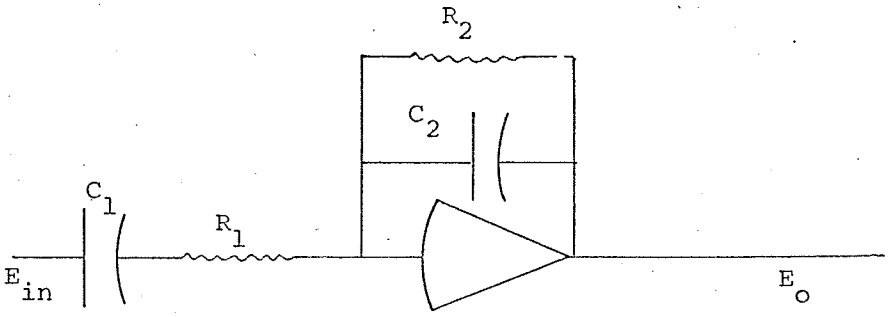

Figure 23a. Circuit for obtaining the sV_{t2} signal

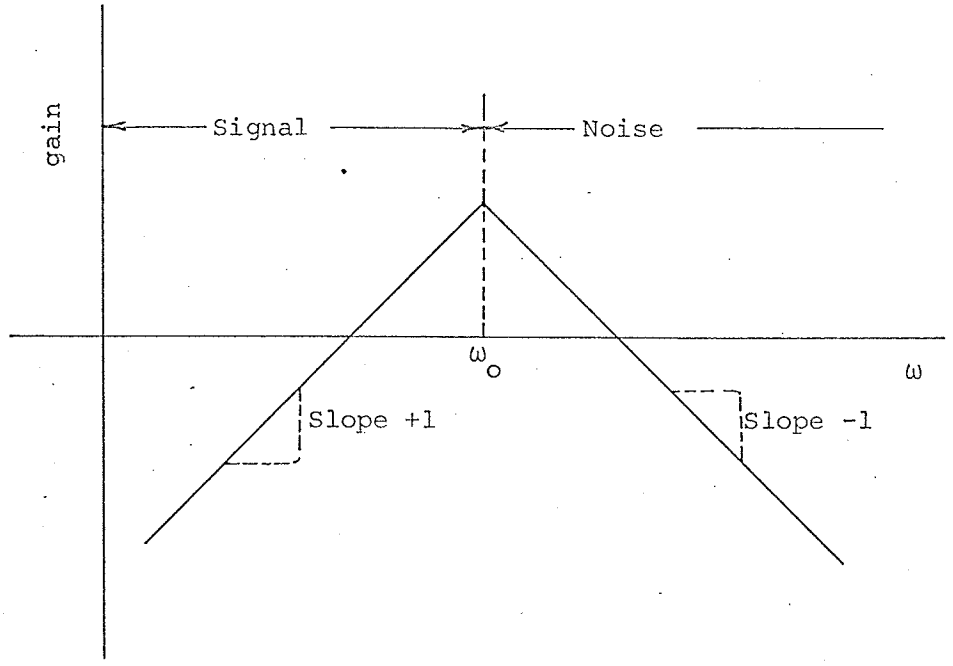

Figure 23b. Bode Plot for circuit which gives the sV_{t2} signal

B. TECHNIQUE FOR OBTAINING THE ACCELERATING POWER SIGNAL

The accelerating power of the machine is the difference between the power output and the power input. Since the losses are not being considered, the mechanical power input should be equal to the electrical power output under steady state conditions. It is not possible to determine the mechanical power input to the machines accurately in practice. However, it is possible to monitor the output power quite easily. Since in the lossless system, the output power is equal to the input power, the input power just before a fault occurs is known. The block diagram shown below illustrates how the accelerating power signal is derived using the above assumptions.

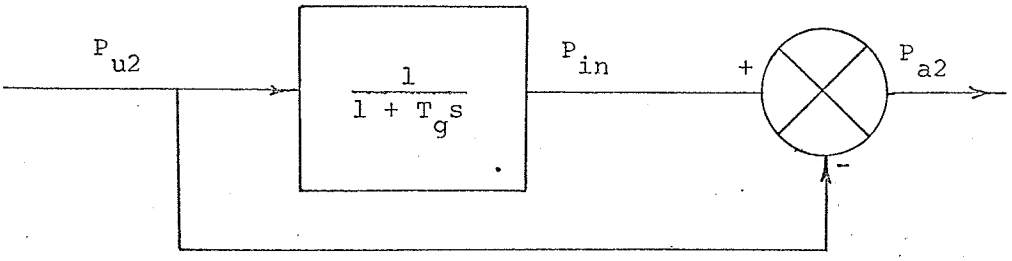

The P_{in} is initially equal to P_{u2} the output power so that the accelerating power P_{a2} is zero. When a disturbance occurs the output power P_{u2} changes but the input power P_{in} remains constant at the pre-fault value because of the large time constant T_g which represents the delay in the governor system. Thus the approximate accelerating power at any instant can be obtained.

C. ****CONTINUOUS SYSTEM MODELING PROGRAM****

PROBLEM INPUT STATEMENTS

```
* THREE MACHINE SYSTEM MODEL
PARAM KVT=3.0E-04
PARAM PAP=0.
PARAM PI1=117.5E06
PARAM PI2=117.5E06
PARAM DELTO1=1.0895
PARAM DELTO2=1.1039
PARAM VFO1=175.87
PARAM VFILO2=115.06
PARAM RIFO1=211.73
PARAM RIFO2=207.46
PARAM VB=18.0E03
PARAM VINP2=23.9085,XT1=0.153,XT2=0.597,XT=0.75
PARAM TDO=5.1,M=.03E06
PARAM TP=.02,KP=1.E-08
PARAM TE1=3.42
PARAM GAIN1=29.
PARAM VREF1=116.
PARAM XDTT=0.2375,XQTT=0.262
PARAM TQOTT=0.089,TDOTT=0.042
PARAM XD=1.32,XQ=0.772
PARAM XDT=0.352,XQT=0.772
      VDB1=VB*SIN(DELTA1)
      VQB1=VB*COS(DELTA1)
      VDB2=VB*SIN(DELTA2)
      VQB2=VB*COS(DELTA2)
* NETWORK SOLUTION AT THE MACHINE TERMINALS
      A1=XT1+XT2+XD
      B1=XT2*COS(DELTA2-DELTA1)
      A2=XT2*COS(DELTA2-DELTA1)
      B2=XT1+XT2+XD
      E1=XT2*(EI1+EI2*COS(DELTA2-DELTA1))
      E2=XT2*(EI1*COS(DELTA2-DELTA1)+EI2)
      D1=VQB1*(XT1+XD)+E1
      D2=VQB2*(XT1+XD)+E2
      DENOQ=A1*B2-A2*B1
      NUMQ1=D1*B2-D2*B1
      NUMQ2=A1*D2-A2*D1
      VQTB1=NUMQ1/DENOQ
      VQTB2=NUMQ2/DENOQ
      R1=XT1+XT2+XQ
      S1=XT2*COS(DELTA2-DELTA1)
      R2=XT2*COS(DELTA2-DELTA1)
      S2=XT1+XT2+XQ
      U1=VDB1*(XT1+XQ)
      U2=VDB2*(XT1+XQ)
      DENOD=R1*S2-R2*S1
      NUMD1=U1*S2-U2*S1
      NUMD2=R1*U2-R2*U1
      VDTB1=NUMD1/DENOD
      VDTB2=NUMD2/DENOD
```

```
* STATE OF THE MACHINES
      VTB1=SQRT(VQTB1**2+VDTB1**2)
      VTB2=SQRT(VQTB2**2+VDTB2**2)
      ID1=(EI1-VQTB1)/(XT1+XD)
      IQ1=VDTB1/(XT1+XQ)
      VD1=XQ*IQ1
      VQ1=VQTB1+XT1*ID1
      VT1=SQRT(VD1**2+VQ1**2)
      ID2=(EI2-VQTB2)/(XT1+XD)
      IQ2=VDTB2/(XT1+XQ)
      VD2=XQ*IQ2
      VQ2=VQTB2+XT1*ID2
      VT2=SQRT(VD2**2+VQ2**2)
      PU1=VD1*ID1+VQ1*IQ1
      PU2=VD2*ID2+VQ2*IQ2
      PU=PU1+PU2
      PI=PI1+PI2
      QU1=VQ1*ID1-VD1*IQ1
      QU2=VQ2*ID2-VD2*IQ2
      QU=QU1+QU2
* DAMPING OF THE MACHINES
      F1=TDOTT*(XDT-XDTT)*VDB1**2/(XDT+XT)**2...
      +TQOTT*(XQT-XQTT)*VQB1**2/(XQT+XT)**2
      F2=TDOTT*(XDT-XDTT)*VDB2**2/(XDT+XT)**2...
      +TQOTT*(XQT-XQTT)*VQB2**2/(XQT+XT)**2
* SOLUTION OF THE MECHANICAL EQUATIONS OF THE MACHINES
      Z1=M/F1
      Z2=M/F2
      Y1=(PI1-PU1)/F1
      Y2=(PI2-PU2)/F2
      DEDOT1=REALPL(0.0,Z1,Y1)
      DEDOT2=REALPL(0.0,Z2,Y2)
      DELTA1=INTGRL(DELTO1,DEDOT1)
      DELTA2=INTGRL(DELTO2,DEDOT2)
* EXCITATION SYSTEM OF THE MACHINE WITH AMPLIDYNE EXCITATION
      VPT1=VT1/120.
      VFB1=VPT1
      VERR1=VREF1-VFB1
      VINT1=GAIN1*VERR1
      VOUT1=LIMIT(-27.,27.,VINT1)
      VFIN=24.4*VOUT1
      VF1=REALPL(VFO1,TE1,VFIN)
      RIF1=REALPL(RIFO1,TDO,VF1)
      IFC1=4.15*RIF1
      EI1=19.55*IFC1
```

```
* EXCITATION SYSTEM OF THE MACHINE WITH STATIC EXCITATION
      VPT2=VT2/120.
      VFIL2=REALPL(VFIL02,.01,VPT2)
      VFB2=.45*.19*VFIL2
      VREF2=.41*VINP2
      VERR2=VREF2-VFB2-KVT*DVT+PAP*PACC
      VINL2=100.*VERR2
      VONL2=LIMIT(-22.,22.,VINL2)
      VF2=34.*VONL2
      RIF2=REALPL(RIF02,TDO,VF2)
      IFC2=4.15*RIF2
      EI2=19.55*IFC2
* STABILIZER SIGNALS
      DELOMG=REALPL(0.0,TP,DEDOT2)
      PACT=PI2-PU2
      PACC=REALPL(0.0,TP,PACT)
      DVTFB=DERIV(0.0,VT2)
      DVT=REALPL(0.0,TP,DVTFB)
      PACTS=PI-PU
      PACCS=REALPL(0.0,TP,PACTS)
      PTFB2=DERIV(0.0,PU2)
      PTFB=REALPL(0.0,TP,PTFB2)
      QTFB2=DERIV(0.0,QU2)
      QTFB=REALPL(0.0,TP,QTFB2)
      PTFBS=DERIV(0.0,PU)
      PTFBS2=REALPL(0.0,TP,PTFBS)
      QTFBS=DERIV(0.0,QU)
      QTFBS2=REALPL(0.0,TP,QTFBS)
PRTPLT DELTA1,DELTA2
PRTPLT PU1,PU2
RANGE PU1,PU2,VF1,VF2,VT1,VT2
TIMER DELT=.01,FINTIM=5.0,PRDEL=.05,OUTDEL=.05
METHOD RKSFX
END
PARAM KVT=0.
PARAM PAP=1.0E-07
END
STOP
```

D. LIST OF SYMBOLS

D_1, D_2	Damping factors of machines 1 and 2 respectively
E_{i1}, E_{i2}	Internal voltage of machines 1 and 2 respectively
G.P.G.	Gate Pulse Generator
H	Inertia constant
I_d, I_q	Projections of the stator current on the axes of the machine
I_{d1}, I_{q1}	Projections of the stator current on the axes of machine 1
I_{d2}, I_{q2}	Projections of the stator current on the axes of machine 2
I_{da1}, I_{qa1}	Projections of the line current on the axes of machine 1
I_{da2}, I_{qa2}	Projections of the line current on the axes of machine 2
I_{f1}, I_{f2}	Field current of machines 1 and 2 respectively
K_a	Gain for the accelerating power signal
K_p	Gain for the active power derivative signal
K_q	Gain for the reactive power derivative signal
K_v	Gain for the voltage derivative signal
K_w	Gain for the speed error signal
M	Inertia constant
P_a	System accelerating power
P_{a1}, P_{a2}	Accelerating power of machines 1 and 2 respectively
P_i	System power input
P_{i1}, P_{i2}	Power input to machines 1 and 2 respectively
P_u	System active power output
P_{u1}, P_{u2}	Active power output of machines 1 and 2 respectively
Q_u	System reactive power output
Q_{u1}, Q_{u2}	Reactive power output of machines 1 and 2 respectively

s	Laplace transform variable
T_{do}', T_{qo}'	Direct and quadrature axis open circuit transient time constant of the machine
T_{do}'', T_{qo}''	Direct and quadrature axis open circuit subtransient time constant
V_b	Equivalent infinite bus voltage
V_d, V_q	Projections of bus bar voltage on axes of machine
V_{d1}, V_{q1}	Projections of terminal voltage of machine 1 on its axes
V_{d2}, V_{q2}	Projections of terminal voltage of machine 2 on its axes
V_{db1}, V_{qb1}	Projections of infinite bus voltage on the axes of machine 1
V_{db2}, V_{qb2}	Projections of infinite bus voltage on the axes of machine 2
V_{dm}, V_{qm}	Projections of terminal voltage on the axes of machine
V_{dtb1}, V_{qtb1}	Projections of terminal bus voltage on the axes of machine 1
V_{dtb2}, V_{qtb2}	Projections of terminal bus voltage on the axes of machine 2
V_{f1}, V_{f2}	Field voltage of machines 1 and 2 respectively
V_{fd}	Field voltage of the machine
V_{go}	Internal voltage of the machine
V_R	Reference voltage of the machine
V_{Ref1}, V_{Ref2}	Reference voltage of machines 1 and 2 respectively
V_t	Terminal voltage of the machine
V_{t1}, V_{t2}	Terminal voltage of machines 1 and 2 respectively
V_{te}	Error in the terminal voltage of the machine
x_d, x_d', x_d''	Steady state, transient, and subtransient direct axis reactance
x_q, x_q', x_q''	Steady state, transient, and subtransient quadrature axis reactance
x_t	External reactance between machine terminals and the infinite bus

x_{t1}	Reactance of transformers at sending end
x_{t2}	Reactance between sending end terminal bus and infinite bus
δ	Angular position of the internal voltage of the machine with respect to the infinite bus
δ_1	Angular position of the internal voltage of machine 1 with respect to the infinite bus voltage
δ_2	Angular position of the internal voltage of machine 2 with respect to the infinite bus voltage
ϕ_{fd}	Field flux linkage
θ_1, θ_2	Power factor angle of machines 1 and 2 respectively

BIBLIOGRAPHY

[1] A.S. Aldred and G. Shackshaft, "The effect of a Voltage Regulator on the Steady and Transient Stability of a Synchronous Generator," IEEE Proceedings, August 1958, pp. 420-427.

[2] A.S. Aldred and G. Shackshaft, "A Frequency Response Method for the Predetermination of Synchronous Machine Stability," IEE Proceedings, August 1959, pp. 2-10.

[3] A.L. Blythe and J.W. Skooglund, "An improved Computer Program for Electric Utility Stability Studies," CEA Fall Meeting, Regina, October 1965.

[4] A.L. Blythe, H.M. Ellis, J.E. Hardy, and J.W. Skooglund, "Dynamic Stability of the Peace River Transmission System," IEEE Trans. Power Apparatus and Systems, Vol. PAS-85, June 1966, pp. 586-596.

[5] A.L. Blythe, "The Effects of Static Excitation Characteristics on System Stability," CEA, Winnipeg, March 1967.

[6] A.L. Blythe and R.M. Shier, "Field Tests of Dynamic Stability using a Stabilizing Signal and Computer Program Verification," IEEE Trans. Power Apparatus and Systems, Vol. PAS-87, February 1968, pp. 315-332.

[7] R.L. Bolger and H.E. Lokay, "Effect of Turbine Generator representation in System Stability Studies," IEEE Trans. Power Apparatus and Systems, Vol. PAS-84, October 1965, pp. 933-942.

[8] D.B. Breedon and R.W. Fergusson, "Fundamental Equations for Analog Studies of Synchronous Machines," AIEE Transactions, June 1956, pp. 297-306.

[9] H.E. Coles, "Dynamic Performance of a Turbo Alternator Utilising 3-term governor control and voltage regulation," IEE Proceedings, Vol. 115, February 1968, pp. 266-279.

[10] P.L. Dandeno, A.N. Karas, K.R. McClymont, and W. Watson, "Effect of High Speed Rectifier Excitaiton Systems on Generator Stability limits," IEEE Trans. Power Apparatus and Systems, Vol. PAS-87, January 1968, pp. 190-201.

[11] J.L. Dineley, A.J. Morris, and C. Preece, "Optimized Transient Stability from Excitation Control of Synchronous Generators," IEEE Trans. Power Apparatus and Systems, Vol. PAS-87, August 1968, pp. 1696-1705.

[12] H.M. Ellis and J.E. Hardy, "Peace River EHV Transmission System Stability and other Technical considerations," Manitoba EHV Symposium, September 1966.

[13] E.E. Hattan, H.D. Hunkins, G.E. Martin, and F.R. Schleif, "Excitation Control to Improve Power line Stability," IEEE Trans. Power Apparatus and Systems, Vol. PAS-87, June 1968, pp. 1426-1434.

[14] W.G. Heffron and R.A. Phillips, "Effect of a modern Amplidyne Voltage Regulator on Underexcited Operation of Large Turbine Generators," AIEE Transactions, August 1952, pp. 692-697.

[15] IEEE Power Generating Committee, "Computer Representation of Excitation Systems," IEEE Summer Power Meeting, Portland, Oregon, July 1967.

[16] G. Manchur, K.R. McClymont, R.J. Ross, and R.J. Wilson, "Experience with High Speed Rectifier Excitation Systems," IEEE Trans. Power Apparatus and Systems, Vol. PAS-87, June 1968, pp. 1464-1470.

[17] D.W. Olive, "New Techniques for the Calculation of Dynamic Stability," IEEE Trans. Power Apparatus and Systems, Vol. PAS-85, July 1966, pp. 767-777.

[18] A.R. Scott, "Optimization of Generator and Excitation System Parameters for Grand Rapids Development," CEA Western Zone Meeting, March 1963.

[19] E.M. Scott, "Influence of Optimized Generator Parameters on the Grand Rapids Transmission System," CEA Western Zone Meeting, March 1963.

[20] K. Vongsuriya and Y.N. Yu, "Steady State Stability Limits of a Regulated Synchronous Machine Connected to an Infinite System," IEEE Trans. Power Apparatus and Systems, Vol. PAS-85, July 1966, pp. 759-767.